Majodina *et al. Miner Miner Mater* 2023;2:13
DOI: 10.20517/mmm.2023.23

Minerals and Mineral Materials

Review

Open Access

Towards improvement of hydroprocessing catalysts - understanding the role of advanced mineral materials in hydroprocessing catalysts

Siphumelele Majodina, Olwethu Poswayo, Tendai O. Dembaremba, Zenixole R. Tshentu

Department of Chemistry, Nelson Mandela University, Gqeberha (Port Elizabeth) 6031, South Africa.

Correspondence to: Dr. Tendai O. Dembaremba, Department of Chemistry, Nelson Mandela University, Building 13 University Way, Gqeberha (Port Elizabeth) 6031, South Africa. E-mail: Olsentodds@gmail.com

How to cite this article: Majodina S, Poswayo O, Dembaremba TO, Tshentu ZR. Towards improvement of hydroprocessing catalysts - understanding the role of advanced mineral materials in hydroprocessing catalysts. *Miner Miner Mater* 2023;2:13. https://dx.doi.org/10.20517/mmm.2023.23

Received: 17 Aug 2023 **First Decision:** 21 Sep 2023 **Revised:** 9 Oct 2023 **Accepted:** 19 Oct 2023 **Published:** 30 Oct 2023

Academic Editors: Wencai Zhang, Feifei Jia, Shaoxian Song **Copy Editor:** Dong-Li Li **Production Editor:** Dong-Li Li

Abstract

Mineral materials play a pivotal in heterogeneous catalysts as active, support, or promoter components, with the oil refinery industry being one of the biggest beneficiaries. While conventional hydroprocessing catalysts have historically met the industry's needs, the growing need to accommodate unique feedstocks, meet the increasing demand for environmentally acceptable products, obtain better product specifications, enhance selectivity for reactions to increase ratios for certain product cuts, and use more cost-effective and abundant mineral materials, has recently motivated for fresh considerations in the development of hydroprocessing catalysts. Based on periodic trends, noble metals possess the most desirable qualities, but their relative abundance in the Earth's crust is too low to meet industry needs. They are costly and highly sensitive to sulfur poisoning. Mo and W lie in the sweet spot, but it is anticipated that they cannot meet the increasing demand. Investigations of electronic interactions of more economical and abundant metals, such as Nb, V, and Fe, with other elements and support materials have yielded a better understanding of synergistic effects that help to access noble metal-like qualities. This work contrasts conventional hydroprocessing catalysts and recently improved catalysts, detailing the chemistry considerations behind the selection of mineral materials used in the catalysts. It also explores how further manipulation of these mineral materials and synthesis approaches is driving toward more desirable properties. The work brings to the attention of the readers the challenges and opportunities for the further improvement of hydroprocessing catalysts to ensure environmental sustainability while meeting the industry's growing needs.

Keywords: Hydroprocessing, hydrodesulfurization, hydrodenitrogenation, hydrodeoxygenation, hydrodemetallization and hydrocracking

INTRODUCTION

The ability of humans to interact with their environment was greatly enhanced with the advent of exploiting mineral materials in our ecosystem during the stone, bronze, and iron ages, defining key functional points of the earliest evident civilizations based on the abilities to modify and add certain characteristics to these materials through various treatments. Human reliance on mineral materials continues, with most modern advancements, manufacturing, and processing relying on mineral material catalysts. The hydroprocessing industry is one such prominent industry where different kinds of catalysts are required at numerous stages to access various products[1,2]. The growth of the petroleum refinery is attributed to be the biggest driver of the growth of the global catalyst market, which is expected to grow to USD 9.5 billion by 2027[2]. These catalysts are mostly different combinations of transition metal silicates, phosphates, carbonates, sulfates, sulfides, nitrides, carbides, phosphides, borides, oxides, and hydrides, with various other elements such as phosphorous, boron, and fluorine being added to improve catalyst properties. Mineral materials, such as alumina, zeolites, titania, cerium, and zirconia, are also crucial as catalyst support materials[3]. Research for improving catalysts for these processes remains a prominent and active area of study[1]. Improved catalysts can reduce refinery costs, improve selectivity for certain products, allow non-conventional feedstock, such as creosotes, to be accommodated, and make them economically attractive fuel sources[4].

While the relative abundance of mineral materials used for current hydroprocessing catalysts is generally not a problem, the increasing demand for petroleum products and the need for more active and highly selective catalysts to improve refinery processes will change this situation. There is also a tendency to incline towards the noble metals, which have demonstrated superiority among all active elements. Research seeks to bridge the gap by manipulating properties of more abundant elements (e.g., iron) to achieve the same level of efficiency to ensure sustainability[5]. The pursuit of improvements in this field is broad, including changes in support materials, improved synthesis protocols, and the incorporation of multifaceted compositions that result in better catalyst properties. On the same note, the importance of recycling spent catalyst materials and the environmental concerns associated with the discarding of the modified mineral materials must also be stressed enough[6]. Sufficient studies are also required to understand the impact of modified mineral materials used in hydroprocessing catalysts on the environment.

Performances of conventional hydroprocessing catalysts used in typical hydroprocessing reactions are discussed, articulating the roles played by the various constituents of the catalysts that are obtained from a wide array of typical mineral materials. Chemistry aspects that motivated the combinations of choice mineral materials used in the conventional hydroprocessing catalysts are discussed. Their limitations (e.g., poor activity for some reactions, poor product selectivity, and catalyst deactivation) are also discussed, and we proffer solutions through this review work. The superiority of noble metals is identified throughout all the discussions, emphasizing the aim to manipulate combinations of more affordable and abundant mineral materials to achieve similar desirable properties. The current position in the development of catalysts to overcome challenges associated with the growing need to accommodate hydroprocessing of unconventional feedstocks, such as creosotes and bio-oils, with examples of promising catalysts, is also well covered.

HYDROPROCESSING IN GENERAL

Hydroprocessing reactions

Hydroprocessing reactions seek to modify the hydrocarbon composition to achieve desirable fuel specifications and eliminate heteroatoms to protect the environment and downstream processes[3,7]. Reactions such as the addition of hydrogen to carbon-carbon double bonds (hydrogenation), breaking of

C-C bonds (hydrocracking), hydroisomerization, reforming, and polymerization are required to upgrade feedstocks, such as heavy oils and oil residues, to meet fuel specifications, including lower boiling points[8]. Heteroatom elimination reactions are known as catalytic hydrotreating reactions, include removal of sulfur, nitrogen, oxygen, and metal, and are referred to as hydrodesulfurization (HDS), hydrodenitrogenation (HDN), hydrodeoxygenation (HDO), and hydrodemetallization (HDM), respectively[9]. HDS and HDN reaction mechanisms [Figure 1] are representative of the reaction mechanisms behind hydroprocessing reactions.

Hydroprocessing reaction competitions

Hydroprocessing reactions occur simultaneously, competing with each other, usually causing a retarding effect on each other[4,10]. Equilibrium constants for the competition of catalyst sites by the heterocyclics generally increase in the order of aromatic hydrocarbons < sulfur compounds < oxygen compounds < nitrogen compounds. HDN is generally more difficult compared to other hydroprocessing reactions that occur simultaneously, with an inhibitory competitive effect, and can be used to dictate the hydrotreating operating conditions[11-14]. For example, high N content (> 60 ppm) negatively affects the ability to achieve deep HDS (less than 10 ppm wt. S)[13,15]. The competitive behavior in the adsorption of heterocyclic compounds on the active sites of hydroprocessing catalysts results in differences in selectivities and reaction depths of the catalysts[15-18]. Different sites for cleavage of C-S, C-O, C-N, and other reactions are also proposed[11]. The need to establish the different sites associated with specific reaction selectivities has created several research questions that have aided the conceptualization of various strategies for improving the catalysts based on composition or design for specific or multiple reactions[11]. Catalyst stacking technologies are also being used to maximize the complementary participation of different catalysts and their different active sites to obtain high performances for multiple reactions[19]. Improved catalysts can reduce the cost of refining crude oil, especially creosotes and other synfuels, making them economically attractive fuel sources[4].

Traditional hydroprocessing catalysts

Hydroprocessing catalysts are usually made up of different combinations of active metals, promoter metals, support materials, and other additives that help improve catalyst properties. Catalyst activity increases with an increasing percentage of active metals up to a certain point where the activity will start decreasing. As such, there is a need to balance between the increasing cost of catalysts as the percentage of active metal increases and the benefits of obtainable catalyst activity[11,20]. Transition metal sulfides are the most prominent materials in hydroprocessing catalysis[21]. The traditional catalysts for hydrotreating are the sulfided combinations of alumina-supported Mo or W promoted by Co or Ni; $CoMo/Al_2O_3$, $NiMo/Al_2O_3$, and $Ni(Mo)W/Al_2O_3$ being the most common commercial examples[19,22]. They are considered the baseline catalysts for benchmarking the performance of potential catalysts. Environmental concerns and the need to accommodate harsher feedstock and shape products have been the main drivers for the continuous development of hydroprocessing catalysts[19,23,24]. These subjects are discussed in greater depth in our previous review[25].

Periodic trends of metals in hydroprocessing

Electronic properties of the selected metals used in the catalysts lay the foundations for understanding catalyst activity and selectivity. Pecoraro and Chianelli[26-29] carried out transition metal tests on HDS activity [Figure 2A], while Eijsbouts[26-29] carried out similar tests on HDN [Figure 2B]. All the studies confirmed that the primary effect for activity is electronic and is related to the position the metals occupy in the periodic table. For both processes, transition metals occupying the first row in the periodic table are relatively inactive, while those occupying the second and third rows have high activity. HDS conversion levels are high for Ru, Os, Ir, Rh, and Re, respectively, while HDN conversion levels are high for Ir, Os, Re,

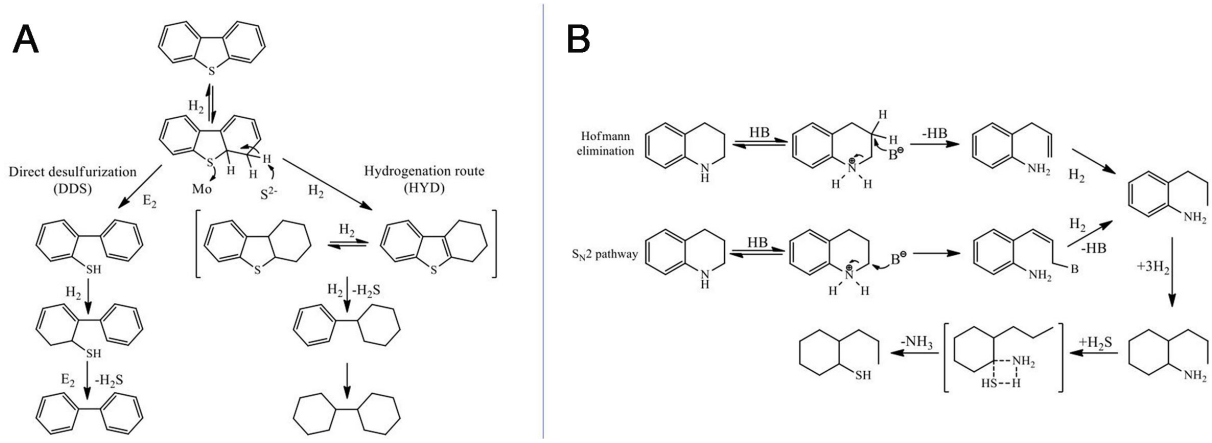

Figure 1. Schematics showing (A) HDS and (B) HDN reactions of typical sulfur and nitrogen containing compounds as representative hydroprocessing reactions. DDS: Direct desulfurization; HDN: hydrodenitrogenation; HDS: hydrodesulfurization; HYD: hydrogenation.

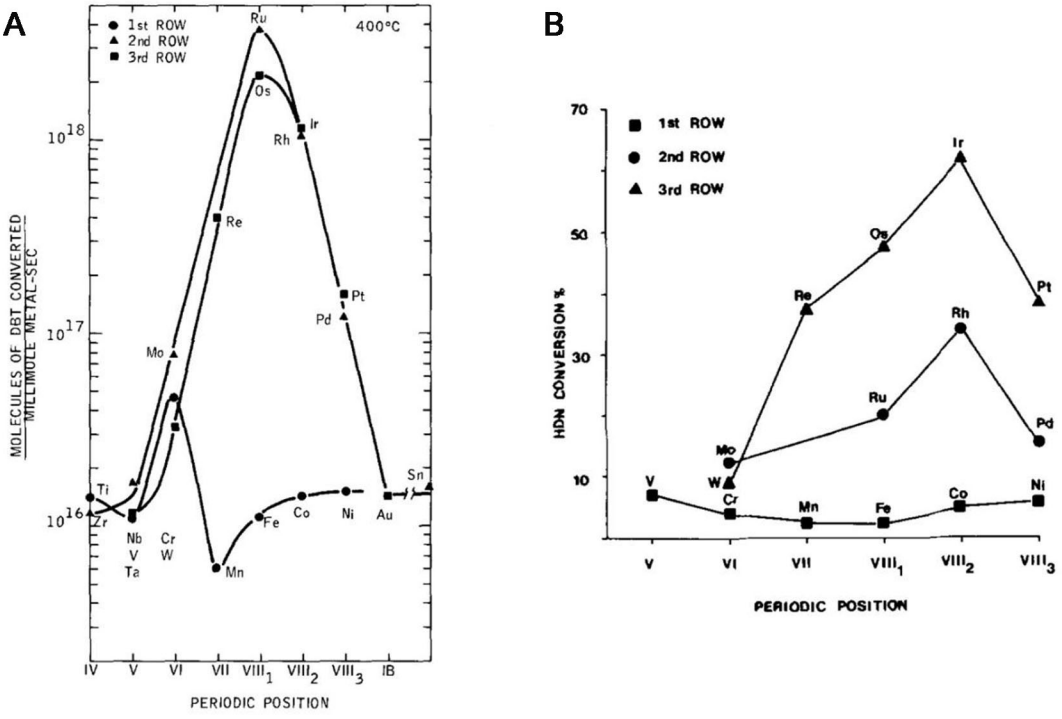

Figure 2. Periodic trends for (A) conversion of dibenzothiophene; (B) conversion of quinoline. Reprinted from references[26-28,31] and[26-28,31] with permission from Elsevier.

Pt, and Rh, respectively. The HDN maxima were found to be at V, Rh, and Ir for the first-row, second-row, and third-row elements, respectively[29]. First-row carbon-supported transition metal sulfides had low quinoline conversions with a minimum at Mn/C and Fe/C and maxima at V/C and Ni/C, while the second- and third-row transition metal sulfides had their minimum with Mo/C and W/C, and the maxima at Rh/C and Ir/C. Noble metal catalysts (Rh/C, Pd/C, Os/C, Ir/C, and Pt/C) show the highest activities and selectivity for propylcyclohexane in quinoline HDN[28]. Raje *et al.* also reported similar volcano plots when they tested second-row unsupported transition metal sulfides: Zr, Nb, Mo, Ru, Rh, and Pd sulfides in the

HDS, HDN, and HDO of coal-derived naphtha that contained significant amounts of S-, N-, and O-containing compounds[30]. Reactivities followed the order: Ru > Rh > Mo > Pd > Zr > Nb, and RuS_2 emerged as the best catalyst for all the processes. Selectivities for hydrogenation *vs.* hydrogenolysis have also been mapped, highlighting the importance of the position of the metals on the periodic table[31]. Observations are that W, Pt, Ir, and Ru are highly selective for hydrogenation.

Understanding periodic trends has motivated the manipulation of electronic properties of various active phases through the use of additives (halogens and phosphorus), chelating ligands, and promoters to facilitate catalyst preparation or performance, usually targeting the use of more affordable metals to obtain noble metal-like characteristics[20].

ROLES OF MINERAL MATERIALS AS SUPPORT MATERIALS IN HYDROPROCESSING CATALYSTS

Catalytic supports play a crucial role in dispersing deposited metals, increasing surface stabilization against deactivation processes such as agglomeration, improving the morphology of the active sulfide component[32], providing beneficial characteristics towards reactions such as defect sites, and enhancing the charge transfer ability and hydrogen spillover[33]. Catalyst supports can also provide additional functional sites and stabilize catalyst active sites. A new active phase on the surface of the catalyst may be formed via the interaction of the support with the catalyst. The following characteristics need to be considered when choosing hydroprocessing support materials: mechanical and thermal stability, surface area, acidity, and porosity[34,35]. The composition and distribution of Brønsted acid and Lewis acid sites are also important[36,37]. Brønsted acid sites are important for promoting the dispersion of the active metal, reducing the reduction temperature of the active metal, and modulating the interaction between the support and the metals. Lewis acid sites are regarded as adsorption sites of the heteroatomic compounds, and they play a role in selectivity *via* hydrogen spillover effects. Supports function differently depending on the strength of their acid sites, and optimal acidity is required for the activity and selectivity of reactions[38]. Metal oxides, such as Al_2O_3, SiO_2, ZrO_2, TiO_2, and CeO_2, and carbon materials have been investigated as hydroprocessing catalyst supports[32,35,39].

Support materials form the basis of hydrocracking reactions with the Brønsted acid sites and play a crucial role in the activity and selectivities of the catalysts[40]. Co-Mo/MCM-41 showed a high yield to the skeletal isomerization reactions because of its strong surface Brønsted acidity and relatively low hydrogenation activity compared to Ni-Mo/MCM-41 and Co-Mo/c-Al_2O_3, which exhibited the low selectivity to the isomerization reactions owing to their high hydrogenation activities[41]. Table 1 summarizes the properties of typical support materials that have been used in hydroprocessing catalysts.

Alumina supports

Alumina supports are the most widely used in industrial applications since they are inexpensive and readily available, with good chemical and thermal stability and excellent surface area. However, the main challenge is its strong interactions with the active metals, which negatively affects catalytic activity[51,52]. During the synthesis of the catalysts, the impregnated metal precursors, Co/Ni(Mo/W), interact with the support, and the high affinity of Ni^{2+}/Co^{2+} ions coordinating with the Al^{3+} surface vacancies can lead to the formation of strongly bonded spinel-like $NiAl_2O_4$ structures, resulting in low catalytic activity due to limited availability of Ni ions to form the active phases Co(Ni)Mo(W)S[52]. Mo_2C, MoS_2, PtO_2, Pt/C, Pd/C, Ru/C, and Rh/C, sulfided Pt/C and sulfided Pt/γ-Al_2O_3 were compared in the HDN of pyridine, and Pt/γ-Al_2O_3 was the most active[53]. The catalysts followed the trend: Pt/C > Pd/Al_2O_3 > Pd/C > Ni_2P > $Pt_{20}Ru_{10}$/C > Pt/Al_2O_3 in the conversion of pyridine[54]. HDO activity using Pt was influenced by the type of support used, showing the

Table 1. Typical hydrotreating supports

Support	Synthesis methods	Mass composition	Surface area ($m^2 \cdot g^{-1}$)	Acidity composition (@200 °C)		Comments	Ref.
				LASs	BASs		
SBA-16 and Al-Ti-SBA-16	Two-step method	Al_2O_3 (0%-10%) and TiO_2 (10%)	975.7 and 969.6	21.4 and 83.7	21.9 and 26.7	Highly ordered structure and enhancing acidity.	[42]
TiO_2-Al_2O_3 (Ti/Al 0-4)	Pre-hydrolysis co-precipitation method	Ti/Al ~0, 0.96, 1.93, 3.88	250.8	Weak acid sites (~65.3), moderate acid sites (~58.5), and strong acid sites (~12.4)	-	Ti modification can modulate metal support interaction, Al-O-Ti bonds formed, and reduced acid sites. Ti enhanced HYD and CUS.	[34]
TiO_2-Al_2O_3	Solvent evaporation-induced self-assembly method	Ti ~0, 10, 20, 40%	428, 391, 365, 296	Weak acid sites ($\mu mol \cdot g^{-1}$) (~196) and strong acid sites (~68)	-	20% support increase of TiO_2 increased pore size, decreased strong acid sites.	[43]
TiO_2-Al_2O_3	EISA method	Ti/Al 0, 0.2, 0.4, 0.6	241, 273, 284, 207	Weak acid sites ($mmol \cdot g^{-1}$) ~0.082 Medium and strong acid sites ~0.022	-	Highly ordered structure with high surface area, narrow pore size distribution, and high stability, Ti-O-Al bonds formed, Ti and Al homogeneously distributed.	[44]
-γ-Al_2O_3-HZSM-5 -γ-Al_2O_3-MCM-41	Physically blending method	HZSM-5 (5%, 10%, 20%), MCM-41 (5%, 10%, 15%)	215	0.33 ($\mu mol \cdot m^{-2}$)	0.49 ($\mu mol \cdot m^{-2}$)	Higher surface area, increased BAS/LAS obtained.	[45]
C@γ-Al_2O_3	Chemical vapor deposition	-	259, 249, 207	Total acidity 315 ($\mu mol \cdot g^{-1}$)	-	Higher dispersion of the active metal and promotion of MoS_2 by Co.	[46]
NPC@γ-Al_2O_3	Pyrolysis of phytic acid and urea impregnated on γ-Al_2O_3	0.7 g of phytic acid, 0.7 g of urea	220	57 ($\mu mol \cdot g^{-1}$)	0.48 ($\mu mol \cdot g^{-1}$)	High electron donating effect of N and P; decreased acid sites on the support.	[47]
Zeolite-activated carbon (ZAC50%)	Reflux	50wt.% activated carbon	379	-	-	Uniform mesoporous structure, moderate acidity, and better active metal dispersion.	[48]
SBA-15, activated carbon, mesoporous alumina	So-gel, commercial activated carbon	-	573, 447, 276	-	-	SBA-16, AC showed a high surface area; the mesoporous catalyst showed higher hydroprocessing and hydrocracking activity due to higher pore size and dispersion.	[49]
Hexagonal mesoporous silica [Ti-HMS (Si/Ti 20, 40, 60)]	Post-synthesis method	-	285	-	-	Ti-incorporation improved the catalytic activity, and Ti-HMS (Si/Al 20) showed more dispersion of the active phase.	[50]
Pseudoboehmite	Eco-friendly technology (reprecipitation) and hydrothermal treatment	-	192	-	-	Bimodal pore distribution. Catalyst supported on H1 has more CoMoS phase.	[35]
Mesostructured titania	-	-	-	-	-	Higher specific surface area.	[51]
Al_2O_3-CeO_2	Sol-gel	CeO_2 loadings (0wt.%, 5wt.%, 10wt.%, and 15wt.%	-	-	-	15wt.% CeO_2 loading resulted in 97% DBT HDS conversion and inhibited the formation of $NiAl_2O_4$ spinnel and increased BAS.	[52]

BASs: Brønsted acid sites; EISA: facile evaporation-induced self-assembly; LASs: Lewis acid sites.

trend: Pt/Al_2O_3 > Pt/ASA > Pt/TiO_2 > $Pt/CeZrO_2$ > Pt/ZrO_2 > Pt/CeO_2[55]. However, coke formation was cited as the biggest challenge with these catalysts[56]. While the traditional alumina-supported catalysts do well for HDO, alumina is unstable in the presence of high levels of water and is highly vulnerable to coking due to the acidic sites[24].

Mesoporous silica supports

Mesoporous silicas have excellent physicochemical properties, such as high surface area, large pore size, and structural order[39,42,57]. Silicas provide moderate metal-support interaction and well-dispersed active metals, resulting in good catalyst performance[58]. The textural properties of SBA-15 are desirable for HDS of refractory sulfur compounds, including stability under harsh hydrotreatment conditions[57]. Liu *et al.* investigated NiMo catalysts supported on SBA-15 and -Al_2O_3 for the HDS of 4,6-DMDBT and found good dispersion of active metals and high HDS activity compared to -Al_2O_3-supported catalysts[58]. SBA-16 promoted good dispersion of active metals and is reported to be good for hydrogenation catalysts with large pores that promote mass transfer[42]. Hydrocracking properties of Pd (1%) loaded mesoporous silicas (MCM-41, MCM-48, SBA-15 ASA) were investigated, and a cracked product distribution was found to decrease with loss of mesopores while low metal dispersion resulted in overcracking due to long poor residence time of olefins[59]. However, the low acidity of mesoporous silicas limits their range of application as catalytic supports[57].

Titania, zirconia and ceria supports

Titanium dioxide has been widely used in hydroprocessing catalysts and is reported to promote better dispersion (e.g., of MoS_2) and increased acidity[36,56]. However, conventional TiO_2 has not penetrated commercial applications as much as alumina because it suffers low mechanical strength and specific surface area[51,60]. Several strategies have been developed to obtain TiO_2 with better pore sizes and specific surface area, but crystallization during preparation leads to the collapse of the porosity[46]. Better HDS reactivity by weakening the geometric constraint through dealkylation and/or isomerization has been reported through TiO_2 and ZrO_2[61]. TiO_2 and ZrO_2 have been reported to be ideal as HDO catalysts. Sudhakar *et al.* found that these supports provide additional HDO sites, stabilize the catalyst active sites, and enhance resistance to coking[22]. Cerium dioxide (CeO_2) is one of the most abundant rare earth metals and has attracted attention due to its properties such as chemical stability. It shares many similar properties with TiO_2[62]. CeO_2 has good chemical stability, can play a role as a promoter, can activate H_2, and promotes the effective dispersion of the active metal. Rare earth metals generally have less carbon deposition, and CeO_2 has a lower tendency for coke formation[63,64]. It is particularly valuable for HDO due to its ability to generate oxygen vacancies and activate H_2 and C=O bonds[56]. However, it is worth noting that CeO_2 is relatively expensive and has low surface area and poor thermal and mechanical properties[39]. Good acidity for C=O bond activation has been reported in TiO_2, ZrO_2, and CeO_2, and the order of their acidity follows the order TiO_2 > ZrO_2 > CeO_2[56]. Small surface area, lack of porosity, and deactivation at high temperatures have been cited as challenges in these metal oxides, encouraging the use of aluminosilicates[56].

Zeolite supports

Hydrated aluminosilicates (zeolites), such as NaY, SAPO-11(34), USY, and ZSM, are gaining more attention as supports due to their good balance of Bronsted and Lewis acid sites, good crystalline structure and controlled porosity, high thermal and mechanical resistance, ease of dispersing active phases optimally, and large surface area[65]. Much attention towards them has increased due to their high isomerization and cracking activities[34,66]. They play an important role in the morphology of the active phase[66]. Y-zeolites are more dominant in commercial hydrocracking applications, while ZSM-5-type materials are preferred for hydrodewaxing or shape-selective cracking[67]. Zeolite desilication was found to improve the performance of a PtPd/HY catalyst in the hydrocracking of a plastic pyrolysis oil/vacuum gas oil blend[68]. Drawbacks with

zeolites include limited pore accessibility and distribution, diffusion barriers, and deactivation by coking[65,69]. Sometimes, strong Bronsted acid sites in zeolites lead to unwanted over-cracking of hydrocarbons and carbon deposition. To mitigate these challenges, various metals, such as Ni, Pt, Rh, Re, La, Bi, Mg, K, and Mg non-metals, such as P and B, have been incorporated in the support[43,66,70-74]. Ga was found to be the most suitable[43,61,75]. Zhou *et al.* demonstrated that Ga weakens the acid site strength on the surface of Y zeolites by acting as a weak electron acceptor compared to Al[66]. Zeolites have also been successfully employed in HDO but also show dealumination and high coke formation[76]. A high acidity and well-balanced ratio of micro- and meso-porosity was found at a higher SiO_2/Al_2O_3 ratio, giving high activity in a Ni-W/Zeolite-Y catalyst[77].

Carbon material supports

Carbon materials show good thermal conductivity, textural and structural characteristics, weak interaction with active metals, higher dispersion of active metals, higher resistance to coke deposition due to the absence of acidity, lower tendency of nitrogen poisoning, wide transport pores that limit the formation of condensation products during hydrotreating reactions, and good electron transport capability[46,78,79]. However, it is important to note that different types of carbon materials have different characteristics. Pure carbon materials and activated carbon materials have poor mechanical properties, low density, and microporosity, while mesoporous carbon material is known to have a low surface area, low mechanical strength, and bulk density[46]. Multi-walled carbon nanotubes (MWCNTs) have high surface area, high pore volume, relatively high mesopore diameter, and almost complete absence of micropores. MWCNT-supported catalysts were credited to having a low crystallinity that increases the ability to adsorb hydrogen and act as a hydrogen transfer agent during the hydrogen spillover from the active sites to the adsorbed feedstock molecules, resulting in increased HDS and hydrogenation (HYD) activity and reduced N-containing compound inhibition[32]. Carbon-supported catalysts have lower HDO activity for carbonyl, carboxyl, and methoxyl groups compared to alumina-supported catalysts[24].

Improved support materials

Various strategies have been used to improve support materials and enhance the performance of hydroprocessing catalysts[32]. Changing the support preparation method, use of novel precursors, additives, and chelating agents, blending different support materials, and other modification methods have been used to overcome challenges such as strong metal-support interactions[80]. Various support materials have been mixed together to explore the combination of positive characteristics from these individual materials and overcome their drawbacks. These combinations include TiO_2-Al_2O_3, Al_2O_3-SiO_2, TiO_2-ZrO_2, TiO_2-SiO_2, MCM-41-Al_2O_3, USY, ZSM-5, Ti-SBA-15, MCM-41, Ti-HMS, TiO_2-MgO, Al_2O_3-MgO, CeO_2-Al_2O_3, Al-SBA-15, Al-SBA-16, SiO_2-ZrO_2, SiO_2-TiO_2, Al_2O_3-B_2O_3, and SiO_2-MgO. Additionally, composite materials have been developed, including alumina-carbon, alumina-carbon nanofiber alumina-graphene, alumina-carbon nanotube, zeolite-carbon, and zeolite-carbon nanofiber[32,35,48,58,60,63,80-83].

Silica-alumina-supported NiMo, CoMo, and NiW catalysts show higher HDN, hydrocracking, and hydrodearomatization activities compared to alumina[84]. Much higher hydrocracking activity has been reported through amorphous oxide supports such as amorphous silica-alumina compared to crystalline supports such as zeolites[67]. Reducible metal oxides (TiO_2, CeO_2) have been used as electronic and structural promoters to improve the catalytic activity, selectivity, and thermal stability of the catalysts[63]. Incorporation of Ti can improve the dispersion of the active metals; it can donate electrons to the conductive band of the active metal, weakening the metal-oxide interaction and making it easier to sulfide, and also weakens the metal-sulfur bond energy forming more coordinatively unsaturated sites (CUS) that increase catalytic activity[42,85,86]. The incorporation of Al and Ti in mesoporous silica SBA-15 improves the acidity on the surface[57]. Increasing Si/Al molar ratios (up to 20) in Al-modified SB-15 supported NiMo catalyst resulted

in increasing 4,6-DMDBT HDS activity owing to good dispersion of active metals[36,42,87]. TiO_2-Al_2O_3 has superior HDN catalytic performance due to excellent hydrogen transfer capacity and suitable acid properties[51,88]. Better dispersion of CoMoS was obtained on a TiO_2-SBA-15 composite, resulting in higher DBT and 4,6-DMDBT selectivity and conversion[51]. Ceria has been incorporated into alumina to produce a material with a higher surface area, increased thermal resistance, reduced carbon deposition, improved dispersion of metals on the surface, and better interaction between the active metal and the support[64]. CeO_2 promotes the HDN activity of Ni_2P[64]. Xia *et al.* conducted a study on CoMo/γ-Al_2O_3 catalysts modified with Ce, and they concluded that the introduction of Ce adjusted the acidity properties of the support, formed new BAS and increased the BAS/LAS ratio, resulting in excellent isomerization performance[85]. A carbon/zeolite composite with attractive properties from both materials was reported[38]. The addition of halides (especially F and Cl), P, and B to support materials has also been reported, usually to improve support acidity[9,89]. Promotional attributes are also given to these additives, with improved HDS and HDN activity in conventional catalysts and enhanced hydrogenolysis and cracking in hydrocracking catalysts[90]. Rare earth elements (La, Ce, Nd, and Pr) have been used to modify the acidity of Y zeolites ($SiO_2/Al_2O_3 \approx 25$)[89].

Considerations for catalyst preparation methods and the nature of the precursor components also need to be made. He *et al.* employed three different synthesis methods (impregnation, co-precipitation, and sol-gel methods) to obtain TiO_2-Al_2O_3 binary oxide composites and found that the catalyst synthesized using the co-impregnation method possessed the highest specific surface area, while the one by the sol-gel method showed higher pore volume and better mesopore distribution[86]. Yan *et al.* demonstrated through NiW-HY + Al_2O_3 and by NiW-Al_2O_3 + HY that the order of metal support combination methods played a crucial role in the performance of catalyst performance when they observed significantly different activities and selectivities[91].

ROLES OF MINERAL MATERIALS AS ACTIVE METALS AND PROMOTERS IN HYDROPROCESSING CATALYSTS

Active and promoter mineral materials in hydrodesulfurization catalysts

Conventional hydrodesulfurization catalysts

Conventional HDS catalysts are obtained through sulfidation of metal oxide precursors, i.e., Mo or W oxides (active metal) promoted by Co and/or Ni supported on a support such as Al_2O_3 and TiO_2. Upon sulfidation, MoS_2 or WS_2 with Ni or Co promoter at the edges are generated as the active phases[38]. Various models are used to describe the active phases and are accorded to belong to either Type I [Ni(Co)MoS I] or Type II [Ni(Co)MoS II]. Type I contains the monolayer MoS_2 that maintains a strong interaction with Al_2O_3 via chemical bonds such as (Ni)Mo-O-Al, forming tetrahedral Mo oxides that are difficult to reduce and sulfide. Type II represents weaker interactions with Al_2O_3 via van der Waals-type interactions with suppressed dispersion, MoS_2 layers with better stacking, increased cathedral Mo oxides that are easier to reduce, and complete sulfidation that leads to better HDS activity[38]. The role of the promoter is to donate electrons, promote dispersion, and reduce the interaction between the support and the metal (active metal)[82]. With a better understanding of the Co(Ni)Mo(W)S structure, it has been widely recognized that the HDS activity can be promoted by tuning the morphology of the active phase, the interaction between the active metal and the support, adjusting the properties of the supports (surface area and porosity, acidity), and using additives and chelating ligands[36].

Metal precursors have been varied during synthesis of HDS catalysts to come up with enhanced catalytic activity. Traditional metal salts are being replaced by other metal precursors, such as ammonium heptamolybdates, and cobalt salts, such as heteropoly compounds (HPCs). Dawson, Anderson, Keggin, and Strandberg HPCs as precursors for CoMo catalysts were found to produce catalysts with higher activity due

to good homogenous distribution of the active phases on the surface of the support and more metal loading compared to conventional compounds[92]. Anderson-type HPCs $\{Mo_{12}O_{30}(\mu 2\text{-}OH)_{10}H_2[Co(H_2O)_3]_4\}$ contain both Co and Mo atoms in their molecular structure, and using them as precursors leads to a higher concentration of active CoMoS phase on the support material and increased HDS activity due to intimate contact between Co and Mo atoms[92]. Various additives have also been investigated to improve the activity and selectivity of conventional HDS catalysts; P, F, B, Cl, Zn, Mg, Li, Na, K, Ca, and rare-earth metals, with P and F being the most prominent[90,93,94].

Improved hydrodesulfurization catalysts

HDS has never been a challenge due to the high reactivity of most S-containing compounds until recently due to the need to achieve deep desulfurization through improved desulfurization of refractory S-containing compounds and the need to accommodate harsher feedstock that have higher concentrations of S-containing compounds, especially the refractory compounds[80,95]. Transition metal phosphides[96], silicides, and carbides, nitrides have been proposed as deep HDS catalysts[95,97]. Carbides have drawn much attention due to their unique catalytic properties for deep HDS such as the resistance to sintering at high temperatures during HDS reactions; they have strong interactions with heteroatoms (S, N) and inertness towards C-C bond scission, resulting in high selectivity, high hydrogenation activity with their noble metal-like catalytic properties[95,98,99]. Doping non-metal atoms into metal phosphides results in the formation of isolated sites and electronic modification that enhances HDS activity and stability[95]. However, metal phosphides suffer from long-term stability and are prone to deactivation due to their strong affinity with the adsorbates, especially at high temperatures[99]. Several authors have shown that transition metal phosphides (MoP, Ni_2P, and Co_2P) as an active phase are found to be one of the active catalysts in HDS catalysts[100]. The Metal phosphide catalysts exhibit higher HYD activities as compared to Co(Ni)Mo(W)S catalysts and possess high catalytic activity in HDS reactions, thus increasing HDS activity[95,97,100]. Ni_2P catalysts display a strong resistance to deactivation by sulfur[38,97]. Cellia *et al.* found that metal phosphides change the acid-base properties of the support, which affects the dispersion of the active phase, resulting in improved catalytic activity[101]. Noble metals (Pd, Pt, Ru, Re, Rh, and Ir) have also been widely investigated for deep HDS catalysis due to their high hydrogenation and hydroisomerization activities, Pd and Pt being the most prominent[36,102,103]. Weise *et al.* compared an unpromoted Pt catalyst with a Pt-doped industrial CoMo catalyst and observed a 46% increase in activity in the latter, attributing the increase in catalytic performance to the incorporation of Pt atoms on the terminal edges and corner sites of CoMo[104]. Pt reduced the binding energy of sulfur, favored the formation of CUS, and created sites that are favorable to the adsorption of sterically hindered molecules such as 4,6-DMDBT[104,105].

We recently reported higher HDS of DBT due to a good synergistic effect between Rh promoter and Mo and more MoS_2/RhMoS phases when we tested a series of RhMo-x/Al_2O_3 catalysts with different chelating ligand ratios (x = ethylene diamine, tetraacetic acid, acetic acid, citric acid)[104,105]. We attributed high activity to electron donation from Rh to the Mo conducting band, weakening Mo-S bonds and facilitating the formation of CUS [Figure 3]. However, the high cost and vulnerability of noble metals discourage their industrial application as HDS catalysts.

More cost-effective and abundant metals to replace the conventional active and promoter metals, especially Mo and W, are also being sought due to the increasing demand, low crust abundance, high mining cost, and environmental toxicity of these metals[36,38,106]. Ti, V, Nb, and Fe have been tested as potential HDS catalysts[36]. Iron has attracted the most attention due to its low cost, high crust abundance, and environmental friendliness[36]. Fe has some level of hydrogenation activity as it is known to have lattice structures and an unfilled d-electron layer, similar to metal species that are used in conventional

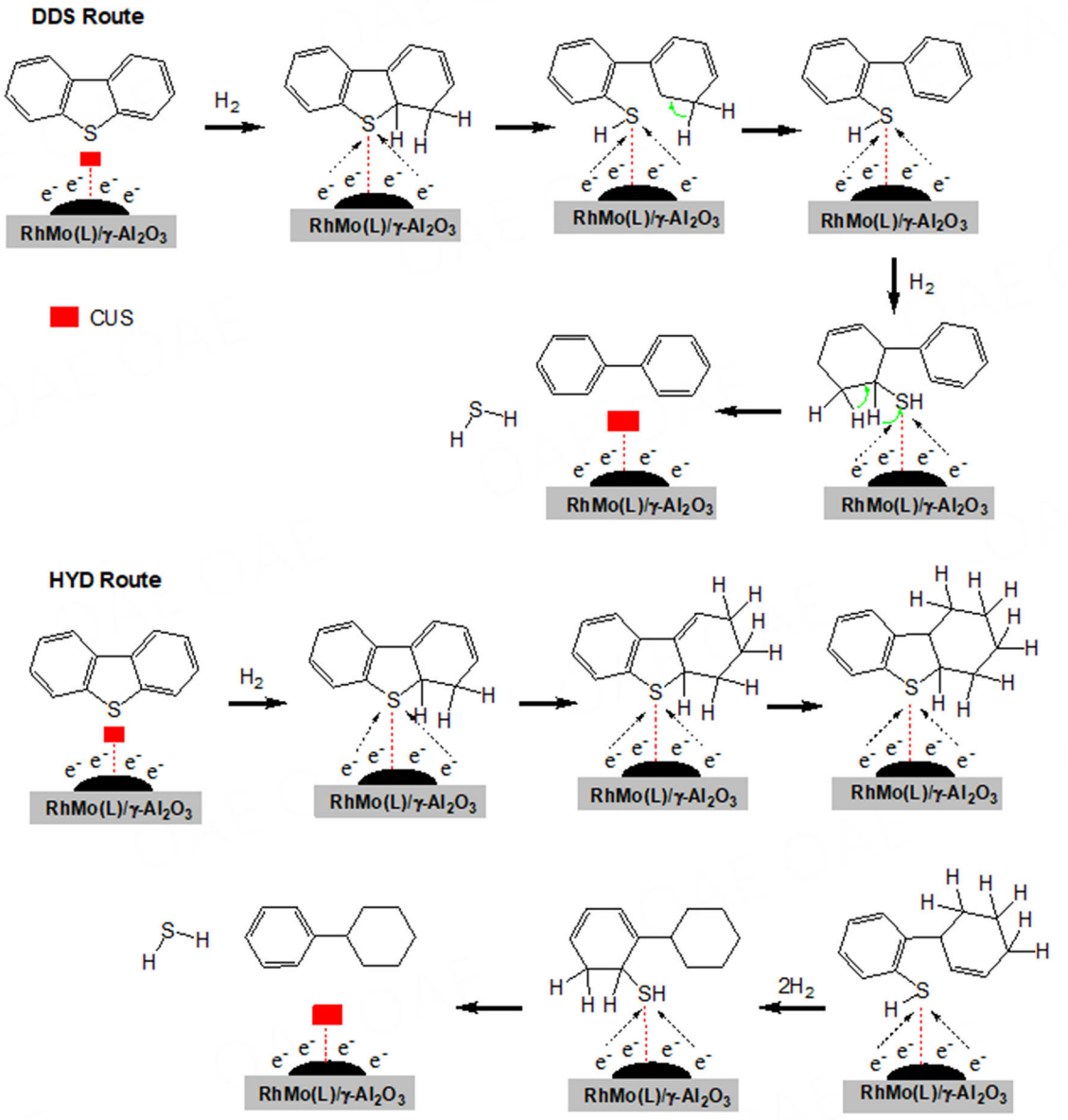

Figure 3. Proposed Mechanisms of DDS and HDS reactions on RhMo chelated Catalysts in HDS of DBT[104,105]. DBT: Dibenzothiophene; DDS: direct desulfurization; HDS: hydrogenation-desulfurization.

hydrotreating catalysts (Co, Ni, Mo, Pt, and Pd)[36]. Although Fe is common in processes such as ammonia synthesis, direct coal liquefaction, Fischer-Tropsch synthesis, and HDO, there are few studies where Fe was tested as an active metal in HDS catalysts. Iron-based catalysts are generally considered to have poor HDS activity, with iron sulfide having much lower than Mo and W sulfide, which is associated with Pauling d% of metals that lead to the different strength of the metal-sulfur covalent bond and sulfidation degree of TMS[36]. Li *et al.* reported improved activity of Fe-based catalysts after incorporating zinc as a promoter[107]. The presence of Zn in the catalyst attributed excellent electron donation to Fe, thereby forming a new active phase (FeZnSx)[95,107]. The addition of Zn also resulted in the generation of more sulfur vacancies[37]. The study also emphasized the major role played by suitable support materials in enhancing the catalytic activity of Fe-based catalysts. It was found that the incorporation of nitrogen on the carbon support provides

unique electronic properties such as promoting the dispersion of Fe, improving its electron-donating capabilities to the active metal (Fe), greatly weakening the Fe-S bond and promoting the formation of CUS, thereby enhancing the HDS activity[95,107]. Typical catalysts that have been developed for HDS are presented in Table 2.

Active and promoter mineral materials in hydrodenitrogenation catalysts

Conventional hydrodenitrogenation catalysts

The C(sp^2)-N bond is very strong and makes hydrogenation of at least the N-heterocyclic ring in aromatic nitrogen-containing heterocycles a prerequisite to achieving C-N bond breaking, unlike in HDS where pre-hydrogenation of the S-ring is a possible pathway but not a prerequisite for C-S bond breaking[93,116-118]. As such, HDN catalysts need to be bifunctional, having both hydrogenation sites and hydrogenolysis sites. The most common HDN catalysts are the conventional Mo and W sulfides promoted by Ni sulfides, e.g., Ni/Mo-Al_2O_3 and Ni/W-Al_2O_3[8,119]. Although these catalysts are prominent in hydroprocessing, their HDN activity is poor[21]. These catalysts require intensive operating conditions to hydrogenate the heterocyclic rings, often causing unnecessary saturation of the carbocyclic rings to achieve C-N cleavage[119]. CoMo, NiMo, and NiW catalysts are significantly more active for HDS than for HDN at any given reaction condition[22]. N-containing compounds are less reactive to hydroprocessing and consume more hydrogen, and the process is more energy-intensive[22]. Higher energies are required to break C-N bonds. Heterocyclic N-containing compounds, such as quinoline and indole, are more difficult to remove, require more severe conditions, and are predominant in heavier feeds[118] HDN becomes more difficult when shifting from light to heavier feeds with higher boiling points and complexity, e.g., shale oil- and coal-derived oils[11,120]. The development of better HDN catalysts becomes even more important considering the growing need to process heavy and low-quality feeds rich in highly refractory N-containing compounds[13,14,121]. Besides that, all acidic catalysts (cracking, reforming, fluid catalytic cracking, hydrocracking, HDS, hydrogenation, and isomerization) are vulnerable to inhibition/poisoning by nitrogen-containing compounds, and good HDN catalysts will be important for HDN pre-treatment of feedstocks[7,13,120,122].

Improved hydrodenitrogenation catalysts

Various transition metal oxides, sulfides, phosphides, borides, nitrides, and carbides have been investigated as HDN catalysts[21,123,124]. Sulfides, nitrides, and carbides show good potential for HDN due to their ability to exchange S, N, or C, and they can adapt their chemical composition to that of the feed during reactions to form highly active phases[125]. Al-Megren *et al.* demonstrated using a pyridine stream that the HDN activities of bimetallic (CoMo) carbide, oxide, nitride, and sulfide catalysts are of the order: $CoMoC_x$ ~ $CoMoN_x$ ~ $CoMoO_x$ > $CoMoS_x$, while their stability follows the order: $CoMoC_x$ > $CoMoN_x$ > $CoMoO_x$ with decrease in activities over time[124]. Qiu *et al.* found the α-phase of Mo_2C to have the highest selectivity and conversion of quinoline compared to the β-phase[126]. Better HDN potential has been demonstrated using metal phosphides, borides, and nitrides. Fang *et al.* investigated the effect of different metals, metal loading, ratio of metal to phosphorous, and other catalyst preparation methods on the activities of transition metal phosphides[21]. The performance of transition metal phosphides was found to be significantly higher than metal sulfides. High activity was obtained from a NiP catalyst, with further improvement of activity being obtained with the addition of small amounts of Co or Fe and a change of support materials[21]. This was attributed to Ni preferentially occupying the active hydrogenation square pyramidal M(2) site[21]. During simultaneous HDS and HDN, the overall activity of metal phosphides followed the order of Ni_2P > WP > MoP > CoP > Fe_2P[13]. Transition metal phosphides were tested for HDS (dibenzothiophene) and HDN (quinoline), and their activities followed the order Fe_2P < CoP < MoP < WP < Ni_2P. Ni_2P/SiO_2 had higher activity compared to the commercial Ni-Mo-S/Al_2O_3 (HDS 98% *vs.* 78% and HDN 80% *vs.* 43%) and commercial Co-Mo-S/Al_2O_3 (HDS 85% *vs.* 80%)[23]. It was also demonstrated that HDN using Ni_2P involves activation at carbon positions α and β to nitrogen atoms in contrast to sulfides where activation only occurs

Table 2. Typical catalysts for HDS reactions

Catalyst	Composition			Feedstock	Reaction conditions	Comments	Ref.
	Active material(s)	Promoter(s)/Additive(s)	Support				
MoS_2	MoS_2	-	-	DBT and/or Q in decane	Batch, 340 °C, 3 MPa H_2 pressure, copper scrubber for H_2S	Strong hydrogenation function, quinoline inhibitory on HDS via hydrogenation pathway.	[108]
$CoMo/Al_2O_3$	Mo	0.57wt.%, 1.21wt.%, 2.18wt.%, 2.68wt.%, 3.35wt.% Co, 8.17wt.%, 8.27wt.%, 8.35wt.%, 8.37wt.%, 8.45wt.% Mo	Al_2O_3	DBT	Batch Parr reactor, 593 K, 1,250 psi, Time on stream = 4 h	Increased activity in Co-promoted catalysts due to cobalt sulfide upon addition of Co/Al_2O_3 to Mo/Al_2O_3 or $CoMo/Al_2O_3$ catalysts. Both MoS_2 and CoMoS phases were promoted.	[109]
$CoMo/Al_2O_3$-TiO_2	MoS_2	13wt% of MoO_3 and 3.3wt% of CoO	Al_2O_3-TiO_2	Pyrolysis gasoline	Fixed-bed, 400 °C, 1 atm	Ti increased the surface acidity and improved the reductive behavior of the tetrahedral and octahedral Mo species. $CoMo/Al_2O_3$-TiO_2 with 10wt.% titania removed over 96% of sulfur-containing molecules in Pygas with improved product quality.	[60]
$CoMoP/\gamma$-Al_2O_3	Mo	12.5wt.% ± 0.2wt.% of Mo, 3.5wt.% ± 0.1wt.% of Co and 1,5wt.% ± 0,1wt.% of P	γ-Al_2O_3	DBT, quinoline and naphthalene	Flow glass reactor, 280 °C, 3.5 MPa, WHSV = 80 h^{-1}	Hydrothermal treatment of a flash calcined gibbsite makes it possible to obtain hydrotreating catalysts with the highest or the same activity in the HDS and HDN of fuel mixture compared to catalyst supported on alumina obtained through the precipitation of pseudoboehmite from aluminum nitrate.	[35]
CoMo/ MWCNT-citr, $CoMoS/Al_2O_3$-citr	Mo	12.0wt.% of Mo and 3.2wt.% of Co, Ctr	Al_2O_3 and MWCT	DBT	Fixed bed, 280 °C, 3.5 MPa, LHSV 20.0 h^{-1}	CoMo/MWCNT-citr catalyst had the highest HDS activity due to higher sulfidation degree, higher CoMoS phase content, and improved dispersion of sulfide components.	[79]
$CoMoS/C@\gamma$-Al_2O_3	MoS_2	3.2wt.% Co and 12.0wt.% Mo	$C@\gamma$-Al_2O_3	DBT	Fixed bed flow, 270 °C, 3.5 MPa, LHSV = 20.0 h^{-1}	Higher dispersion of sulfided components and enhanced promotion of MoS_2 by Co.	[46]
$CoMoS_2$/ZSM-5	MoS_2	Co, 10.7wt% Mo, EDTA	ZSM-5	4,6-DMDBT	High-pressure stirred reactor, 573-593 K, 2-5.0 MPa	Multi-stacked MoS_2 nanocrystallites on $CoMoS_2$ /MZSM-5 provide more available sulfur vacancies to facilitate the DDS pathway and catalyze efficiently the hydrogenation.	[110]
$CoMo/NDC@Al_2O_3$	Mo	18% (mass) MoO_3 and 4% (mass) CoO	$NDC@Al_2O_3$	DBT, 4,6-DMDBT, and Dagang diesel	Batch reactor, 300 and 320 °C, 6 and 7 MPa, LHSV = 1 h^{-1}, H_2/Oil = 200:1	The introduction of NDC reduced the interaction between the support and active components. Improved dispersion of active phase and sulfidation degree of Mo by 21.8% compared to the $CoMo/\gamma$-Al_2O_3.	[111]
Sulfided NiMo /γ -Al_2O_3	8wt.% Mo	3wt.% Ni on	γ-Al_2O_3 (Condea, pore volume 0.5 $cm^3 \cdot g^{-1}$, specific surface area 230 $m^2 \cdot g^{-1}$)	4,6-DMDBT *vs.* presence of 2-methylpyridine and 2-methylpiperidine	Fixed bed, 340 °C and 5 MPa	DDS and HYD inhibited, 2-methylpiperidine > 2-methylpyridine, no significant contribution from change to aromatic solvent	[112]
$NiMo/Al_2O_3$	MoS_2	3.0wt.% NiO and 13.0wt.% MoO_3	Al_2O_3	DBT	Fixed-bed, 240, 260, and 280 °C, 4 MPa, LHSV = 20 h^{-1}	Ni-Al_2O_3 interaction enhances the availability of surface nickel atoms to form more NiMoS phase and improves the microstructure of MoS_2.	[36]

NiMo	MoS_2	Ni	-	DBT	Batch reactor, 340 °C, 50 bar	Both catalysts exhibited good performance (lp-NiMoS, 95.8%, and hp-NiMoS, 98.6% DBT conversion), with hp having the highest due to the formation of more NiMoS.	[113]
NiMo/SBA-15	Mo (6.09wt.%, 10.53wt.%, 11.08wt.%, 15.75wt.%)	Ni (1.65wt.%, 3.04wt.%, 2.59wt.%, 2.63wt.%)	SBA-15	DBT	Batch reactor, 320 °C, 3 and 6 MPa	One-pot synthesis promoted the generation of dispersed shorter MoS_2 slabs with desirable average stacking numbers.	[114]
NiW/Al_2O_3	WS_2	Ni, P WO_3 (20w.t%), NiO(4wt.%) and P_2O_5 (2wt.%)	Al_2O_3	DBT	Fixed-bed, 220-280 °C 4.0 MPa, LHSV = 10-60 h^{-1}	Addition of P improved the availability of surface Ni atoms, P weakened metal support interaction, and enhanced the promotion of NiWS.	[80]
NiMoW/Ti-HMS	MoS_2 and WS_2	3.8wt.%, 13.8wt.% and 17.3wt.% of NiO, MoO_3 and WO_3	Ti-HMS mesoporous	DBT	Batch reactor, 320 °C, 58.6 bar	More CUS formed, increased both DDS and HYD and high dispersion.	[50]
NiTMo-x/Al_2O_3	Mo	Ni, tetradecylamine; for NiO and MoO_3 (3.6wt.% and 16.9wt.%, and 3.5wt.% and 16.8wt.%)	Al_2O_3	4,6-DMDBT	Fixed-bed, 360 °C, 4.0 MPa, LHSV = 15.0 h^{-1}, time on stream = 6 h	NiTMo-2.0/Al_2O_3 had the most corner and edge S vacancies, exhibited the highest reaction rate constant, and had the highest DDS ratio of 99.5% in HDS of 4,6-DMDBT.	[86]
Ni_2P@C, Ni_2Si@C, and NiS_2@C	-	P, Si	Carbon	DBT	Trickle fixed-bed, 260 and 360 °C, 3.0 MPa	HDS activity: Ni_2P@C > Ni@C ≈ Ni_2Si@C > NiS_2@C. Ni_2P@C shows outstanding stability during the long-term reaction.	[95]
Ni_2-xRuxP/SiO_2	-	Ru, Ni	SiO_2	4,6-DMDBT	Fixed bed, 533-593 K, 3.0 MPa	$Ni_{1.85}Ru_{0.15}P/SiO_2$ catalyst 15 and 6 times more active (on a mass basis) than Ni_2P/SiO_2 and Ru_2P/SiO_2 catalysts. Ru resulted in P surface enrichment and lowered the temperature of precursor reduction.	[97]
Rh-M-P (M = Ru, Pt, Ir)	Rh (5.0 and 4.85wt.%), Pt	Ru (0.15wt.%), Pt (0.28wt.%), Ir, P (5.0wt.%, 1.51wt.%, and 3.0wt.%)	SiO_2	Th and 4,6-DMDBT	Fixed bed, 350 °C, 0.1 and 4.0 MPa	Rh-Pt-P catalyst had the highest HDS activity among Rh-M-P catalysts.	[115]
Pt-Co-Mo	Mo	Pt, 16wt.% Mo and 3.5wt.% Co	-	Diesel	Fixed bed, 355 °C, 30 bar, LHSV = 1.5 h^{-1}, Time on steam = 24 h	The addition of ppm levels of Pt to a conventional Co-Mo-S catalyst boosted HDS activity by up to 46%. Pt is suggested to reduce the sulfur binding energy and increase the abundance of CUS. Pt is speculated to create sites for favorable adsorption of sterically hindered molecules.	[104]

CUS: Coordinatively unsaturated sites; DBT: dibenzothiophene; DDS: direct desulfurization; HDN: hydrodenitrogenation; HDS: hydrogenation-desulfurization; HYD: hydrogenation; LHSV: liquid hourly space velocity; MWCT: multi-walled carbon nanotube; WHSV: weight hourly space velocity ; 4,6-DMDBT: 4,6-dimethyldibenzothiophene.

at the β position. HDN activities of silica-supported phosphide catalysts (Co_2P/SiO_2, MoP/SiO_2, WP/SiO_2, $CoMoP/SiO_2$, and $NiMoP/SiO_2$) were tested using o-methylaniline, and MoP/SiO_2 was found to have the highest activity[127]. Wagner *et al.* showed that of the Ni phosphide phases, HDN activity of quinoline increases in the order Ni_2P > Ni0 > $Ni_{12}P_5$[128]. Transition metal borides were also found to have good hydrogenation activity and strong resistance to sulfur,

making them good candidates for HDN of N-containing compounds[129]. Rhenium sulfide was found to have the highest HDS and HDN rates compared to Rhenium nitride and Re metal. ReN_2 was found to have better HDN activity compared to HDS, but its surface transformed back the Re metal after the reaction[130]. MoN was found to be about an order of magnitude more active than a commercial sulfided Co-Mo/Al_2O_3 in the HDN of pyridine with higher selectivity for C-N hydrogenolysis compared to C-C hydrogenolysis[131]. Lee *et al*. reported rapid hydrogenation of quinoline over Mo_2N[132].

Based on periodic trends in Figure 2B, noble metals are the best candidates for HDN activity. Their high HDN activity is accompanied by a lower tendency for coke formation at milder conditions compared to sulfided CoMo catalysts[24]. Additionally, synthesis of noble metal catalysts with non-alumina supports is easy, where alumina has to be avoided[24]. Noble metals are, however, very expensive, and they are vulnerable to inhibition and/or poisoning[120]. For example, good HDN activity has been reported for a Pt catalyst, but sulfur inhibition has been cited as a major challenge[8]. Contrastingly, alumina-supported metallic Ni, Rh, and Ru showed high HDN activity but suffered deactivation due to H_2S, except for Pt, which maintained suitable activity[133]. HDN of quinoline was very high using 1% Ir in Al- and Ga-modified silica catalysts due to Ga and Al having Bronsted and Lewis acid sites that work in synergy to give high activity alongside the good dispersion of the catalytic sites[134]. However, appreciable deactivation was observed in the catalysts. On the other hand, ReS_2 was among the most active transition metal sulfides, but its activity was not always better than industrial CoMo/Al_2O_3 and NiMo/Al_2O_3, and the promoting effect of Co and Ni was found to be low compared to the Mo catalysts[135]. The addition of $Ru_3(CO)_{12}$, a precursor to catalysts that cleave C-N bonds in amine transalkylation reactions, to a commercial CoMo HDN catalyst resulted in significantly improved activity[4]. Carbon and nitrogen can be incorporated in interstitial positions (lattice) of early transition metals (groups 4 to 6), resulting in some pure transition metal carbides and nitrides (e.g., Mo and W carbides and nitrides) that have metallic properties that resemble noble metals[93,99]. The addition of carbon was reported to cause higher hydrogenation properties compared to the addition of nitrogen[99]. Transition metal oxynitrides and oxycarbides are reported to act as bifunctional catalysts through their metallic and acidic active sites, and HDN of indole can occur without pre-hydrogenation of the aromatic ring. They are efficient at activating dihydrogen and N-containing molecules[125].

Physical properties of the catalysts, e.g., particle size and porosity, also have an influence on catalyst performance[11]. The morphology of the sulfide material (e.g., curvature and stacking of layers) was found to influence the catalyst activity in bulk metal sulfides such as MoS_2 and WS_2[121]. The order of impregnation of the metal precursors on the support (e.g., Mo then Co or Ni, or vice versa) and calcination was found to have a significant influence on the activity of the final sulfided catalyst. Impregnating with Mo first was found to give catalysts with an invariably higher activity[11,93]. Mixing metals by closely interlinking them using sulfur bonds in HDN catalysts results in a significant increase in activity compared to analogous conventionally prepared catalysts[136]. Table 3 comprises a range of catalysts that have been developed for HDN.

Active and promoter mineral materials in hydrodeoxygenation catalysts

Conventional hydrodeoxygenation catalysts

Conventional alumina-supported CoMo and NiMo catalysts are usually applied in HDO at moderate temperatures (300-600 °C) and high pressure (7-20 MPa)[147]. The oxygen is removed through a series of reactions, such as decarboxylation, saturation of unsaturated compounds, and C=O via hydrogenation, cleavage of C-O bonds *via* hydrogenolysis, and cleavage of heavy molecular weight compounds to lighter molecular weight compounds via hydrocracking[148-150] Hydrocarbon percentage yields were similar in the HDO of waste cooking oil using conventional sulfided catalysts (NiMO/Al_2O_3, CoMo/Al_2O_3, and

Table 3. Typical hydrodenitrogenation catalysts

Catalyst	Composition			Feedstock	Reaction conditions	Comments	Ref.
	Active material(s)	Promoter(s)/Additive(s)	Support				
$CoMo/Al_2O_3$	12.5wt.% Mo	3.5wt.% Co 1wt.% P 1wt.% B	Boehmite HQ102 B produced in China (292 $m^2 \cdot g^{-1}$; pore volume 1,02 $cm^3 \cdot g^{-1}$; pore diameter 140 Å)	Straight-run diesel fuel: 0.383% of S; 192 ppm of N; density of 0,861 g/cm^3; boiling range = 207-380 °C ("GazpromneftOmsk NPZ", Omsk, Russia)	31 cm^3 catalyst mixed 1:2 with SiC, 360 and 370 °C, 3.8 MPa, H_2/feed = 544 nm^3/m^3, LHSV = 2.5 h^{-1}	CoMoS phase content increased with increasing concentration of P, but more than 2wt.% of P leads to a decrease of SSA and pore volume. Increased activity is attributed to increased surface concentrations of P(OH) or B-OH groups, which adsorb N compounds before they migrate to the sulfide active component.	[137]
Nitrided 12.5% Mo/Al_2O_3	Mo	-	γ-Alumina xerogel	0.25wt.% carbazole in xylene	2.0 g catalyst in a stainless steel fixed-bed microreactor, feed flow= 20 mL·h^{-1}, H_2 flow = 74.4 µmol·s^{-1}, 573 K, 10.1 MPa	High hydrogenation activity in carbazole HDN. The activity of the nitrided catalysts for the hydrogenation in carbazole HDN is not related to surface acidity but rather to the reduced molybdenum ions Mo^{2+} and Mo^0 on the surface of the molybdenum nitrided catalysts.	[138]
Bulk molybdenum carbide (Mo_2C)	Mo	-	-	2.5wt.% of indole dissolved in decaline or 0.4wt.% carbazole in o-xylene	0.8 g of catalyst in SiC (SiC/Mo_2C = 5:1), 613 K, 60 bar, H_2/feed ratio of 600 and contact times (t_c) 0.13-1.07 s	High HDN is maintained even in the presence of small amounts of S (50 ppm). Bulk Mo_2C behaves similarly to that of a noble metal catalyst. Direct HDN is predominant during the early conversion percentages, while at high conversions, the HYD route is followed.	[129, 139]
α-MoC_{1-x}	Mo	-	Specific surface area (107.6 $m^2 \cdot g^{-1}$)	-	-	Higher SSA, activity, and selectivity than β-Mo_2C	[126]
Molybdenum carbide (Mo_2C) *vs.* Tungsten carbide (W_2C)	Mo or W	-	-	0.4wt.% of carbazole in o-xylene	Downflow fixed bed microreactor, 553 and 653 K, 6 MPa, H_2/feed ratio of 600, contact times (t_c) = 0.07-0.8 s	HDN via hydrogenation for both catalysts. Both are bifunctional catalysts (hydrogenation and isomerization). Both reactions are more significant in W_2C, but the activity of Mo_2C is higher than that of W_2C.	[140]
Silica-supported nickel phosphide (Ni_2P) and Ni-rich bimetallic phosphide catalysts [25wt.% Ni_2P/SiO_2, $Fe_{0.03}Ni_{1.97}P/SiO_2$ and $Co_{0.1}Ni_{1.9}P/SiO_2$]	Ni or Fe or Co	P (ratio 0.9 to 1.0 with metal)	Silica (Cab-O-Sil, M7D)	1,000 ppm carbazole + 500 ppm dodecane in 39.85wt.% p-xylene/decane or 3,000 ppm benzothiophene + 1,000 ppm carbazole + 500 ppm dodecane in 39.55wt.% p-xylene/decane.	0.25 g catalyst mixed with quartz flakes to a total volume of 5 mL in a fixed bed continuous flow reactor, 548-673K, 3.0 MPa, feed flow = 5.4 mL·h^{-1}, H_2 flow = 50 mL·min^{-1}	Higher carbazole HDN conversion in all catalysts compared to commercial Ni-Mo/Al_2O_3. Metal phosphides are much higher (92%-98%) *vs.* Ni-Mo/Al_2O_3 (75%-84%). Carbazole HDN on metal phosphides inhibited by DBT co-feeding Ni_2P/SiO_2 and Ni-rich bimetallic phosphide catalysts maintained their activities. Metal phosphides favored ring-opened and ring-contracted products, indicating the presence of metal and Brönsted acid sites on the catalyst surfaces.	[141]
Transition-metal phosphides (Co_2P, Ni_2P, MoP, WP, CoMoP, NiMoP)	Ni or Mo or W	Ni or Co, P	-	o-propylaniline in n-octane	0.05-0.4 g catalyst diluted with 8 g SiC, continuous-flow microreactor, 643 K, 3 MPa	MoP and WP > Ni_2P and NiMoP > Co_2P and CoMoP. All catalysts except for WP lost their activity in the presence of H_2S, being irreversible in the case of Ni_2P.	[142]

$CoMoP/Al_2O_3$ and $NiMoP/Al_2O_3$	Mo	Co or Ni	Al_2O_3	-	-	NiMoP has stronger hydrogenating power than CoMoP.	[143]
Zeolite supported Nickel phosphides (NixPy)	5wt.% Ni	P (3:0 P/Ni)	Commercial Na^+Y and NH_4^+Y zeolites (Molecular sieves, powder, Si/Al ratio: 2.56) or zeolite (SiO_2/Al_2O_3 mol ratio: 30:1, powder form)	1 mL 10vol.% (14.1wt.%) quinoline in dodecane solution	50 mg catalyst in 1 g of silica gel in 6 mL stainless steel batch reactors, 400 °C, 40 bar	HDN activity: Ni_2P > Ni0 > $Ni1_2P_5$. The activity of catalysts comparable to commercial 5wt.% Pd/C, $NiCoMo/Al_2O_3$ and $NiMo/CeO_2$ catalysts.	[128]
$Ni_2P/MgAlO$	60% Ni	Phosphorous	MgAlO	1.72% DBT (3,000 ppm S), 0.185% quinoline (200 ppm N), 5% tetralin and 0.5% n-octane in n-tetradecane	Fix-bed reactor, 513 to 613 K, 3.1 MPa, LHSV = 2 h^{-1}, H_2/oil ratio = 1,500 (v/v)	MgO/Al_2O_3 ratios had no influence on the intrinsic activity of Ni_2P. $Ni_2P/MgAlO$ with the MgO/Al_2O_3 ratio of 3 showed the highest activities. 92.6% conversion of DBT at 513 K $Ni_2P/MgAlO$ catalysts. 67.6% conversion of tetralin at 613 K, significantly higher than other catalysts (46.1%-58.6%).	[144]
Ni-rich bimetallic phosphides	Mo and Ni	P	-	2wt.% quinoline and 1wt.% DBT in decalin	Simultaneous HDN (quinoline) and HDS (DBT) in a fix-bed reactor. 1 g catalyst mixed with 9 mL quartz sand, 320-380 °C, 3 MPa, WHSV = 6 h^{-1}, H_2 /feed flow ratio of 500:1	Increase in HDN and HDS conversions with increasing temperature, approaching 90% and 100% at 380 °C, higher than the commercial $MoNiW/Al_2O_3$ catalyst. $Mo_{0.05}Ni_{1.95}P$ showed the highest activity in simultaneous HDS and HDN compared to $Co_{0.05}Ni_{1.95}P$, $Mo_{0.05}Ni_{1.95}P$, $Fe_{0.05}Ni_{1.95}P$ and $W_{0.05}Ni_{1.95}P$. Catalyst activity is greatly reduced by quinoline.	[21]
NiB alloy	87.2% of nickel	7.1% of boron	-	0.08% carbazole (100 ppm N) or 0.08% carbazole and 0.17% 4,6-DMDBT (300 ppm S) in o-xylene.	Down-flow fixed-bed microreactor, simultaneous HDN/HDS (0.8 g catalyst) or HDN alone (0.2 g catalyst) in SiC (1:5), H_2 flow = 60,360 $cm^3 \cdot min^{-1}$	Carbazole HDN takes place mainly on the Ni metallic phase, with bicyclohexyl as the main product. Decomposition of catalyst noted during the 100 h of use. Catalyst activity is lower for HDS/HDN due to partial sulfidation of the catalyst.	[129]
W/Al_2O_3	20wt.% WO_3	6wt.% P_2O_5	Al_2O_3 GirdlerT-126, surface area 188 $m^2 \cdot g^{-1}$, pore volume 0.39 $cm^3 \cdot g^{-1}$, particle size 0.15-0.25 mm	Gas oil and pyridine	Flow trickle bed microreactor, 3.5 g catalyst in SiC, LHSV = 8.8 h^{-1}, H_2/ liquid feed of 400 v/v; 598, 623, and 648 K	Simultaneous HDS/HDN. P_2O_5 increases the amount of reducible tungsten oxide species by promoting the formation of octahedral polytungstates, has little effect on the lateral growth of the WS_2 slabs but significantly increases the average number of layers, enhances both HDS and HDN activities but more effectively for HDS than HDN.	[20]
Platinum-doped tungsten carbide (W_2C-Pt)	W	0.3wt% Pt	-	0.17% 4,6-DMDBT (300 ppm S) and 0.08% carbazole (100 ppm N) in o-xylene	350 °C, 6.0 MPa, molar H_2/feed ratio = 600	Simultaneous HDS and HDN. W_2C, Pt-W_2C, W_2C-Pt compared. W_2C-Pt has the highest conversions 55% and 100% of conversion for HDS and HDN, while W_2C, Pt-W_2C are not far at around 27% and 90% for HDS and HDN. Pt increases HDN activity of W_2C-Pt. Increased HDS conversion after t_c > 0.31 s when HDN is complete is attributed to earlier completion of HDN.	[15]

W_2C, Pt-W_2C and W_2C-Pt	W_2C and Pt	-	W_2C synthesized from temperature programmed reaction of WO_3 (Fluka 99.9% pure) with 10vol.% CH_4/H_2 gas mixture.	0.17% 4,6-DMDBT (300 ppm S) and 0.08% carbazole (100 ppm N) in o-xylene	1:5 catalyst SiC, 0.25 g catalyst, 350 C, 6.0 MPa, molar H_2/feed ratio of 600	Simultaneous HDS and HDN. W_2C exhibits both HDS and HDN activity. Addition of Pt showed no effect on HDS activity at short contact time (t_c < 0.21 s), unlike HDN activity, where a significant increase was observed. HDS only increased towards the completion of HDN, indicating possible inhibition of N on Pt. W_2C and Pt-W_2C had similar activity (up to 27% HDS and 90% HDN activity) compared to W2C-Pt (55% HDS and 100% HDN activity). The addition of Pt prior to W_2C synthesis results in no increased activity.	[15]
Re/Al-SBA-15 and Ni-Re/Al-SBA-15	5wt.% Re	1wt.% Ni	SBA-15 572 m^2/g, 0.5^{3}cm /g, Dp 6.96 nm	2.5wt.% of o-toluidine in cyclohexane	Fixed-bed flow reactor system, 4 cm^3 catalyst, 673-723 K, H_2 flow = 50 $cm^3 \cdot min^{-1}$, atmospheric pressure	The highest HDN activity in 5wt% Re/Al-SBA-15(10) is attributed to the fine dispersion of Re over the support and successful incorporation of Al into SBA-15, which enhances the strong metal-support interactions and formation of moderate acid sites. Ni-Re/Al-SBA-15 had higher activity due to Ni promoter effects.	[145]
Mo-Ir/Al_2O_3	Mo	0.34wt.%-0.53wt.% Ir	γ-alumina CS 331-1 SA 255 $m^2 \cdot g^{-1}$, pore volume 0.76 $mL \cdot g^{-1}$, particle size of 0.16-0.32 mm	220 ppm of pyridine and 240 ppm of thiophene.	Fixed bed, 0.05-0.2 g catalyst, 320 °C, 20 bar, H_2 flow = 0.4 $mol \cdot h^{-1}$	Simultaneous HDN/HDS. The addition of Ir to Mo/Al_2O_3 led to increased reducibility of the Mo phase and enhancement of HDN and HDS activities, especially HDN, where a synergetic effect resulted in 3 times more activity at loadings of about 0.34wt.%-0.53wt.% Ir. HDN/HDS selectivity of modified catalysts was higher than the selectivities of individual Ir and Mo catalysts.	[146]
Pt/A1$_2O_3$ and Pt/SiO_2-A1$_2O_3$	Pt	-	Alumina (Condea, Sp - 180 $m^2 \cdot g^{-1}$) or silica alumina (Condea, 40% of SiO_2, Sp - 374 $mE \cdot g^1$)	-	-	Five times more active than NiMo/Al_2SO_3, sulfur inhibition poses a challenge.	[8]

DBT: Dibenzothiophene; HDN: hydrodenitrogenation; HDS: hydrogenation-desulfurization; HYD: hydrogenation; SSA: specific surface area; WHSV: weight hourly space velocity; 4,6-DMDBT: 4,6-dimethyldibenzothiophene.

NiW/Al_2O_3)[151]. HDO of methyl phenols has been achieved using an alumina-supported CoMo catalyst at an even lower pressure of 2.85 MPa and 300 °C[152]. The influence of conventional promoters in driving HDO reactions has also been discussed in the literature, e.g., Co being more HDO selective compared to Ni and octahedral Ni species being more active than tetrahedral Ni species in NiMoS/Al_2O_3[153,154]. Generally, oxygen-containing compounds are highly reactive, but phenols and benzofurans tend to be less reactive, and these are found in higher concentrations in coal-derived oils[7]. The need to migrate from alumina-supported catalysts due to their vulnerability to dealumination, especially for high oxygen content feedstocks such as biodiesel, and the need to effectively hydrodeoxygenate the less reactive phenols and benzofurans has been driving further development of HDO catalysts. Bio-oils of very low sulfur content are also known to cause poor regeneration of catalyst active sites, affecting catalyst performance[155-160]. Leaching of sulfur has also been reported in sulfided

catalysts due to high product water content when applied in high biodiesel, motivating the need to move to sulfur-free or unsulfided catalysts[161].

Improved hydrodeoxygenation catalysts

New non-conventional hydroprocessing bimetallic catalysts, such as alumina-supported Ni-Fe and Ni-Cu, have been reported as promising HDO catalysts[148,162]. Ni-Fe/Al_2O_3 was tested on three model compounds of bio-oil: furfuryl alcohol, benzene alcohol, and ethyl oenanthate at 400 °C, and the conversion was found to be 100%, 95.48%, and 97.89%, respectively. The pathway of C-O cleavage was followed[148]. A synergistic effect of Ni and Cu was attributed to the high HDO efficiency obtained through Cu-Ni/ZrO_2 compared to the monometallic Ni and Cu catalyst[149]. Although monometallic catalysts show a promising route for HDO, bimetallic and trimetallic catalysts are more promising as they have been shown to inhibit the sintering of the active phase due to their exceptional electronic and dispersion properties[149]. HDO and decarboxylation products are obtained in the HDO of vegetable oils when using monometallic Mo/SiO_2 and Ni/SiO_2, respectively, while a mixture of decarboxylation and HDO products are obtained through bimetallic Ni Mo/SiO_2 with overall catalytic activity following the order Ni/SiO_2 < Mo/SiO_2 < NiMo/SiO_2[154]. Similar observations were made in the HDO of rapeseed oil using NiMo/Al_2O_3 > Co/Al_2O_3 > Ni/-Al_2O_3[154]. Xue *et al.* obtained the highest HDO activity on bioderived phenol through the trimetallic alumina-supported Ni-Cu-Co catalyst when they investigated how the activity varies from monometallic, bimetallic, and trimetallic catalysts using alumina-supported Ni, Ni-Co, and Ni-Cu-Co[150]. In contrast, Horáček *et al.* found bimetallic NiMO/Al_2O_3 to be more active than trimetallic NiCoMo and NiCoW catalysts[163].

Numerous HDO catalysts that migrate from traditional alumina supports have been tested. A carbon-supported CoMo catalyst has been studied for the HDO reaction with 4-methyl-acetophenol, guiacol, and ethyl decanoate as a feedstock below the typical HDO temperature range (280 °C) and 7 MPa[164]. Successful HDO of phenols in the temperature range of 300-450 °C and 5 MPa using a MgO-supported CoMo catalyst has been reported[165]. NiW with C support has also been employed for the HDO of phenols at a very low pressure of 1 MPa at a temperature of 250-300 °C, which is lower than the typical HDO temperature range[166]. Yoosuk *et al.* reported an amorphous unsupported NiMoS catalyst with high HDO activity[167]. Unsulfided catalysts on neutral supports, such as activated carbon and SiO_2, have also been explored to address the challenges of very low sulfur bio-oils[155-160].

Noble metals have also been investigated as HDO catalysts, and these are mostly hosted on other supports besides alumina[168]. Pd/Al_2O_3 was reported to be suitable for the *in-situ* HDO of phenol, *o*-cresol, and *p*-*tert*-butylphenol with high selectivity of cyclohexanone and had better conversions compared to Raney Ni catalysts[169]. A C/alumina-supported Ru catalyst was tested for the HDO of pyrolysis oil at 350 °C and 20 MPa[167]. Better hydrocarbon yields have been reported through Pt/Ac catalysts compared to Pt supported on Al_2O_3, Cr_2O_3, and SiO_2[170]. Wildschut *et al.* tested Ru/C, Pt/C, and Pd/C catalysts and proved that the noble metal catalysts have a higher HDO efficiency compared to alumina-supported NiMo and CoMo catalysts with Ru metal catalysts performing better than Pd and Pt[171]. A Pt/Al_2O_3 catalyst has been reported for *in-situ* HDO[55]. Pd supported on activated carbon and Pd nanoparticles were investigated for the HDO of phenol with formic acid under mild conditions, and the study realized that even though the activity of the activated carbon-supported catalysts is better compared to nanoparticles shortcomings included particle aggregation, organic intermediates blocking the active sites, and leaching of Pd[168]. Table 4 summarizes typical catalysts developed for HDO.

Active and promoter mineral materials in hydrodemetallization catalysts

Conventional hydrodemetallization catalysts

While alkali and alkali earth metal salts in feedstock can be easily removed by washing before distillation,

Table 4. Typical hydrodeoxygenation catalysts

Catalyst	Composition			Feedstock	Reaction conditions	Comments	Ref.
	Active material(s)	Promoter(s)/Additive(s)	Support				
$CoMo/Al_2O_3$	Sulfided CoMo	-	Al_2O_3	*o*, *m*, *p*-cresols	Autoclave, 360 °C, 7 MPa and 60 min	The efficiency of the HDO reaction of ortho < meta < para. P-cresol reported 95% conversion, while o-cresol had 87% conversion.	[147]
$CoMo/Al_2O_3$	4% CoO, 15% MoO, 235 $m^2 \cdot g^{-1}$ Al_2O_3	-	Al_2O_3	Phenols (methyl substituted)	Microflow reactor, 300 °C, 2.85 MPa	Two pathways were observed DDO (leading to the formation of aromatics) and HYD (formation of cyclohexane).	[9]
NiMo	Unsupported NiMO sulfide	-	-	Phenol	Parr reactor, 350 °C, 2.8 MPa, 60 min, 150 rpm	NiMo sulfide followed HYD pathway, forming aliphatic hydrocarbons with 96.2% conversion due to the addition of Ni, while Mo sulfide followed DDO pathway.	[167]
$NiFe/Al_2O_3$	15wt.% Ni, 5wt.% Fe	-	Al_2O_3	Furfuryl alcohol, benzene alcohol, and ethyl oenanthate	Tubular reactor, 300-400 °C, atmospheric pressure	A 100%, 95.48%, and 97.89% conversion for furfuryl alcohol, benzene alcohol, and oenanthate was observed, respectively. The byproducts of the reaction include toluene, 2-methylfuran, and heptance. The conversion of oenanthate is more affected by temperature.	[148]
Ni-Cu-Co/Al_2O_3	20Ni-5Cu-5Co/Al, 20Ni/Al, 20Ni-5Cu/Al	-	Al_2O_3	Bio-derived phenol	240 °C, 4 MPa, 6 h	Ni-Cu-Co/Al_2O_3 performs better (100% conversion) than monometallic and bimetallic catalysts (< 80% conversion). The main products of the reaction included cyclohexane and cyclohexanol. Both HDO pathways were illustrated as there was a sign of DDO pathway indicated by the formation of benzene, which is unlikely in situ HDO.	[150]
Cu/Al_2O_3, Ni/Al_2O_3, Cu-Ni/Al_2O_3	60wt.% Cu/Al_2O_3, 60wt.% Ni/Al, 20wt.% Cu-40wt.% Ni/Al	-	Al_2O_3	Furfural	Microbatch reactor, 300 °C, 10 bar/hydrogen donor (methanol/isopropyl)	Bimetallic catalyst Cu-Ni/Al_2O_3 had a better performance when compared to the monometallic analogs of Ni and Cu. Isopropranol is a better hydrogen donor and yields higher conversions compared to methanol.	[149, 162]
Ni/Ce-SBA-15	5wt.% Nickel	Cerium 0.08 Ce:Si ratio	Ce-SBA-15 696 m^2/g, 0.98 cm^3/g, pore diameter 9.3 nm	4wt.% anisole in heptane	Fixed-bed tubular reactor, 200 mg catalyst in SiC, 7 bar, 290 °C	Improved catalytic activity and selectivity towards benzene (double compared to Ni/SBA-15). Ce promotion is more efficient for intermediate Ce content Ce/Si = 0.03. Better performance is also attributed to better dispersion of the metallic phase and formation of specific active sites in the Ni particles in contact with Ce-containing surface species.	[172]
Pd/Al_2O_3*vs.* Raney Ni	3wt.% Pd, Raney Ni: 9:11 (Ni:Al)	-	Pd/Al_2O_3: 250 $m^2 \cdot g^{-1}$ of Al_2O_3, 80-120 mesh	Phenol, *o*-cresol, *p-tert*-butylphenol	Tubular reactor, 470-490 K, 3.5 MPa	Phenol HDO Pd/Al_2O_3 cyclohexanone selectivity: 96.1%, 92.4%, and 71.1%, with methanol, ethanol, and H_2 as hydrogen sources, respectively. HDO of phenol Raney Ni cyclohexanone selectivity: 20.5%, 27.4%, and 12.6%, with methanol, ethanol, and H_2 as hydrogen sources, respectively. Conversions using Pd/Al_2O_3; H_2 > EtOH > MeOH, phenol (82.5%) > o-cresol > p-tert-butylphenol (0.65%). Better HDO of *o*-cresol with EtOH as hydrogen donor as compared to Raney Ni.	[169]
Ru/C, Ru/TiO_2, Ru/Al_2O_3, Pt/C, Pd/C	5wt.% of active metal	-	C	Bio-oil	Batch autoclave, two-stage operating conditions: 250 and 350 °C, 100 and 200 bar, 4 h	Ru/C showed a higher yield of 60wt.% and had better HDO performance (90wt.%) than other noble metal catalysts. Ru/C yields better-upgraded oil than traditional $CoMo/Al_2O$. Pd/C had higher yields than Ru/C, but oil had a high oxygen content.	[171]
Pt/Al_2O_3, Pt/TiO_2,	-	-	Al_2O_3, TiO_2, ZrO_2, SiO_2,	Bio-oil	Autoclave, 350 °C, 6.9 bar	Pt/Al_2O_3 showed better performance compared to other Pt catalysts, reducing oxygen content from 41.4wt.% to 2.8wt.%. Supports influence	[55]

Pt/ZrO_2, Pt/SiO_2-Al_2O_3	SiO_2-Al_2O_3	how well the catalyst performs in HDO

DDO: Direct deoxygenation; HDO: hydrodeoxygenation; HYD: hydrogenation.

heavy metals can only be effectively removed through HDM using catalysts and hydrogen at high temperatures[7,173]. Conventional alumina-supported NiMo, CoMo, and NiW hydrotreating catalysts have been reported for HDM[173,174]. Nickel removal from bitumen-derived and Conradson carbon residue oils was investigated using a commercial $NiMo/Al_2O_3$ catalyst; high Ni removal was achieved under mild conditions[175]. Ancheyta-Juárez *et al.* studied the HDM of Maya heavy crude using $Ni-Mo/Al_2O_3$ catalysts, cited diffusion limitation to the effective processing of large molecules, and recommended high catalyst pore volumes in the range 100-250 Å to be optimal for HDM[176]. Similar pore size ranges were also reported by Liu *et al.* when they tested $Ni-Mo/Al_2O_3$ catalysts on the HDM of Saudi Arabia vacuum residuum[177]. They indicated high HDM activity for the smaller and middle range Ni and V compounds, but effective HDM of the larger compounds required macropores (> 100 Å)[177]. HDM is easy, but the deposition of metal products is a challenge that necessitates considerations for catalyst metal retention capacity, pore structures, size distributions, and acid-base properties of the support and catalyst morphology[7,178]. Organometallic compounds of high molecular weight and dimensions that approach or exceed catalyst pore size also cause fouling of catalysts[179-181]. Metals cause or promote catalyst deactivation as they accumulate on catalyst surfaces through deposition (e.g., as metal sulfides)[181,182]. Fe bound by naphthenates causes plugging when it forms FeS in catalyst beds and filters. FeS also enhances coking reactions[7]. Catalyst activity, selectivity for desired products, and lifespan are influenced. Heavy metals also restrict conditions for the disposal of spent catalysts[181]. Heavy metals are commonly found in porphyrin rings and are mostly concentrated in high boiling point fractions (e.g., heavy oil residues, asphaltenes, and resins), with V and Ni being the most abundant in most oils[7,178,181]. These aspects motivate the continuous development of HDM catalysts, especially since HDM is important as a first step to protect downstream catalysts for cracking, HDS, HDN, and HAD[7,173,174].

Improved hydrodemetallization catalysts

Alumina-supported HDM catalysts are not efficient as they suffer deactivation through the deposition of metals on active sites and pore plugging arising from accumulations of metal sulfides[180]. Rana *et al.* used carbon as a support for HDN and observed that carbon support leads to weak metal support interaction, resulting in more Type II active sites that increase the deposition of metal on the carbon surface, preventing overlaying on existing MoS_2 sites[178]. Rana *et al.* also investigated the incorporation of TiO_2 into alumina to produce a $CoMo/TiO_2$-Al_2O_3 and obtained better textural properties and higher HDS activity but a lower HDM activity, indicating the need for higher average pore diameter and macropore size distribution to achieve higher HDM activity[183]. Rana *et al.* attributed much of the HDM catalysis activity to Mo sites when they tested the promoter effect of Fe, Co, and Ni, observing the trend of Fe > Co > Ni for the promoters[178]. They also investigated the effect of mixing peptized alumina with activated carbon to reduce diffusion limitations of larger compounds such as asphaltenes and enhance the metal storage capacity of the catalysts. Patents are also available for Mo, W, and Fe (with Co, Ni, or Fe promoters) and 1:1 alumina to carbon extrudate support with a bimodal type pore size distribution (i.e., both meso- and macro-porosity), and a magnesium aluminosilicate clay as potential HDM catalysts[184,185]. Typical catalysts that have been developed for HDM are summarized in Table 5.

Table 5. Typical hydrodemetallization catalysts

Catalyst	Composition			Feedstock	Reaction conditions	Comments	Ref.
	Active material(s)	Promoter(s)/Additive(s)	Support				
Commercial NiMo /Al_2O_3	Mo	Ni	Al_2O_3	bitumen-derived heavy oils and Conradson carbon residue	625-685 K, LHSV = 0.14-0.80 h^{-1}, 13.7 MPa), H_2/oil ratio = 890 $m^3 \cdot m^{-3}$	High Ni removal under mild conditions with minor improvements with increasing severity of conditions.	[175]
Ni-Mo/Al_2O_3	Mo	Ni	Al_2O_3	Vacuum residue	410 °C, LHSV = 0.3 h^{-1}, 15 MPa, H_2 to liquid was 600	The percentage of light impurities easier to remove on spherical catalysts (78.20% and 39.43% in HDM and HDCCR reactions, respectively) is higher than 65.20% and 17.50% on cylindrical catalysts.	[186]
Commercial NiMo/Al_2O_3 (B), and NiMo/Al_2O_3 (A) {has high metal content}	Mo	Ni	Al_2O_3	VO-TPP in o-xylene, thiophene	600 K, LHSV = 0.2 h^{-1}, 8.0 MPa	The model results showed that the pore blocking rate in catalyst B was lower than in catalyst A. These data confirm that it is a durable high-performance HDM catalyst.	[187]
Co-Mo/γ Al_2O_3	Mo	Co	γ Al_2O_3	Asphaltenes, diesel, extra heavy oil	360-410 °C, LHSV = 1.0 h^{-1}, 4.0 MPa, H_2/oil ratio = 600 $nL \cdot L^{-1}$	The catalyst synthesized on a carrier with cylindrical pores exhibited higher catalytic activity in sulfur, heavy metals, and asphaltenes removal reactions that are synthesized on a carrier with slit-like pores.	[188]
FeMo, CoMo, NiMo	Mo	Fe, Co, Ni	(0%-75% activated carbon in alumina	residual oil and heavy crude oil (Ku crude)	380-400 °C, LHSV = 1.0 h^{-1}, 120 bar, H_2/Oil = 680	Carbon in support reduced coke and metal depositions on pore-mouth and catalytic sites. The optimum textural and mechanical properties of the support are obtained at a 1:1 carbon-alumina weight ratio. FeMo-supported catalyst composition (10wt.%-75wt.% carbon) had the best HDM results for an optimum pore diameter.	[178]

HDCCR: Hydrodemetallization and continuous catalyst regeneration; HDM: hydrodemetallization; LHSV: liquid hourly space velocity; VO-TPP: vanadium oxide tetraphenyl porphyrin.

Active and promoter mineral materials in hydrocracking catalysts

Conventional hydrocracking catalysts

There are two extreme hydrocracking catalytic functions: an acidic functionality and a hydrogenation/dehydrogenation functionality[189]. The acidic functionality constitutes bond cleavages, isomerizations, and intermolecular and intramolecular skeletal rearrangements, including cyclizations. The acidic functionality is provided by support materials such as silica-alumina, zeolites, or alumina[9,179,190]. Cracking reactions usually require protonic (Brønsted) acid sites[179,190]. The hydrogenation/dehydrogenation functionality has a hydrogenolysis character that cleaves bonds of reactants into fragments, dehydrogenates saturated reactants to produce reactive olefin intermediates, hydrogenates the unsaturated products from cracking, and prevents catalyst deactivation by hydrogenating coke precursors. These two extremes result in different product distributions. The extent of each of these reactions varies from catalyst to catalyst. Hydrocracking catalysts of commercial importance possess dual functionality, with reactions being primarily catalyzed by a strong acidic functionality and a weak hydrogenation/dehydrogenation functionality with minimal hydrogenolysis.

Conventional sulfided hydrotreating catalysts, such as $CoMo/Al_2O_3$ and $NiMo/Al_2O_3$, do not have sufficient protonic acidity to afford good cracking functionality even at high temperatures (400 °C)[179,190]. However, feed pre-treatment using these catalysts is essential to reduce the heteroatomic impurities since hydrocracking catalysts are sensitive to inhibition and/or poisoning[9,191,192]. This pre-treatment also helps with saturation of olefins and aromatics. One of the early successful hydrocracking catalysts was pelleted WS_2[193]. There is also a wide body of literature on hydrocracking tests using traditional hydrotreating NiMo, CoMo, and NiW catalysts[194]. Hydrocracking of poly-aromatic hydrocarbons to mono-aromatic hydrocarbons has been reported using $NiMo/Al_2O_3$-HY and NiMo/Beta catalysts[195]. The use of $CoO\text{-}MoO_3/Al_2O_3$ for hydrocracking of heavy feedstock is common, and promotion of the catalyst with Na, K, or Li has been reported, with Li showing the best results[194].

Improved hydrocracking catalysts

Improved hydrocracking through modified conventional hydrotreating catalysts has been reported[89,196,197]. A Ni (1wt.%, 2wt.%, and 3wt.%) modified sulfated zirconia (SO_4/ZrO_2) catalyst was investigated for hydrocracking activity and selectivity, and the catalyst loaded with 1% Ni had the highest acidity producing the highest activity and selectively for the gasoline range (70.28%)[198]. Bimetallic catalysts have been reported to show better activity[77,199]. Bimetallic $CoWS_2$ catalysts were found to have higher hydrocracking activity compared to monometallic Co_9S_8 and WS_2 catalysts[199]. Bimetallic Ni-W catalysts showed high catalytic activity (78%-91% conversion) compared to monometallic Ni catalysts (74.2%-82.7% conversion)[77]. Hydrocracking of waste plastic pyrolysis oil and vacuum gas oil using a NiW/HY catalyst and plastic pyrolysis oils using a Ni/SBA-15 have been reported[200]. Catalysts constituting multiple metals to fine-tune the bifunctionality have also been reported. Liu *et al.* carried out hydroconversion of polyolefins using $Pt/WO_3/ZrO_2$ and HY zeolites and reported an 85% yield at 225 °C[201]. Pt had the role of activating the polymer followed by cracking on WO_3, ZrO_2, and HY zeolites, which are acid functions ending. WO_3 and ZrO_2 sites were responsible for isomerization, and Pt was responsible for hydrogenation of the olefin intermediates. There is a special category of hydrocracking catalysts called shape-selective catalysts that utilize crystalline aluminosilicates with pore structures of specific geometrical characteristics that restrict access of reactants and products to particular sizes and shapes[189]. A novel class of promising hydrocracking catalysts based on stable single-atom Mo has recently been reported by Sun *et al.*[202]. Good hydrogenation activity, high liquid oil yields, and reduced tendency of coke formation were observed when tested on slurry phase hydrocracking of vacuum residue.

For the hydrogenation/dehydrogenation functionality, metals from Group VIII and VIb are selected based on their hydrogenation capabilities, and noble metals, such as Pt, Pd, and Pt/Re, and transition metals, such as nickel, cobalt, molybdenum, and tungsten, have been reported to be among the best performers[9,67,189]. Pt and Pd have good hydrogenating functions but must be used in an environment that does not have sulfides[203]. Higher hydrogenation and less cracking activity by Pt compared to NiMoS-supported bifunctional catalysts were observed by Brito *et al.* during the hydrocracking of octylcyclohexane[203]. The use of chromium, niobium, and Sn has also been reported but not as extensive[9,67]. Nanoparticles of noble metals and transition metal oxides, nitrides, and carbides have also been reported for the hydrogenation component of hydrocracking catalysts[204,205]. Typical catalysts developed for hydrocracking are presented in Table 6.

SUMMARY AND PERSPECTIVES

Conventional hydroprocessing catalysts [$Co(Ni)Mo/Al_2O_3$ and $Ni(Mo)W/Al_2O_3$] have met the hydroprocessing industry catalyst needs, but better hydroprocessing catalysts are now being highly sought after to meet the increasing demand for petroleum products, achieve stricter fuel specifications, and selectively target individual hydroprocessing reactions to accommodate unique feedstocks and/or obtain

Table 6. Typical hydrocracking catalysts

Catalyst	Composition			Feedstock	Reaction conditions	Comments	Ref.
	Active material(s)	Promoter(s)/Additive(s)	Support				
NiMo/Al_2O_3-HY and NiMo/Beta	Mo (and 15wt.% MoO_3)	Ni (5wt.% NiO)	Al_2O_3-HY and Beta	Tetralin or 1-MN	Fixed-bed reactor, 320-420 °C, 6 MPa WHSV = 2 h^{-1}	NiMo/Beta(25) possessed high Brønsted acidity and high MoS_2 dispersion and can facilitate the conversion of intermediates of 1-MN hydrocracking (mainly methyl tetralins and indanes) into MAHs. NiMo/$A_{30}Y_{50}$ - NiMo/Beta(25) (up to 99.9% conversion of 1-MN and 63.8% selectivity of MAHs). NiMo/$A_{30}Y_{50}$ with 30wt.% Al_2O_3 showed the best performance in selective hydrocracking reactions owing to the high density of MoS_2 and BAS.	[196]
NiMo/γAl_2O_3, NiMo/γAl_2O_3 + Beta	Mo	Ni	γAl_2O_3 and γ Al_2O_3 + Beta	Naphthalene	Fixed bed reactor, 400 °C, 4 MPa	Catalytic performance is dependent on the coupled hydrogenation ability of NiMo/γ-Al_2O_3 and the acidity of Beta zeolite. The highest BTX selectivity (62.8%) at 98% naphthalene conversion in Ni(2)Mo(13.2)/γ-Al_2O_3 + Beta(20) due to well-matched HYD and acid function.	[197]
NiMo/REY + Al_2O_3	Mo	Ni	REY + Al_2O_3	Vacuum gas oil	Fixed bed reactor, 390 and 410 °C, 16.0 MPa, LHSV = 0.7 h^{-1}	A high yield of middle distillates fraction (50.5wt.% at 410 °C) was achieved. Increase in selectivity to middle distillates selectivity can be explained by a decrease in the strong acid site density that suppresses overcracking reactions to produce naphtha.	[89]
NiW/Y-ASA-Al_2O_3	W	Ni	Y-ASA-Al_2O_3	Straight-run gas oil, dimethyl disulfide, and aniline, vacuum gas oil, unconverted oil	Fixed bed reactor, 340-410 °C, 16.0 MPa, LHSV = 1.4 h^{-1}	Increase of zeolite content in the catalysts leads to an increase of activity and a decrease of selectivity to diesel in second-stage hydrocracking. Increased activity is attributed to the increasing BASs.	[198]
$CoWS_2$	W	Co	-	Vacuum residue	Autoclave batch reactor, 693 K, 10 MPa	Bimetallic $CoWS_2$ catalysts have higher activity than monometallic Co_9S_8 and WS_2 catalysts in regard to hydrocracking TOF and C7-ASP conversion for vacuum residue hydrocracking. $CoWS_2$ has well-dispersed mono-slabs with a better dispersion of 11.1 nm and stability.	[199]
Ni/Zeolite-Y, Ni-W/Zeolite-Y and NiW/HY	W (22.7wt.% WO_3)	Ni (4.54wt.% NiO)	Zeolite-Y and HY	Heptane	Batch reactor, 400-440 °C, 80 bar	Higher catalytic activity (conversion, 78%-91%) Ni-W catalysts than Ni-based monometallic catalysts (conversion, 74.2%-82.7%), with NiO-WO_3-ZY30(SiO_2 /Al_2O_3 ratio equal to 30) exhibiting the highest conversion.	[77]
Pd/x (where x = SBA-15, ASA, MCM-41, and MCM-48)	1wt.% Pd	-	SBA-15, ASA, MCM-41, and MCM-48)	n-hexadecane	Packed bed, 473 K, 60 bar WHSV = 10 $g_{n\text{-}C16} \cdot g_{cat}^{-1} \cdot h^{-1}$	All materials (including ASA) exhibited low acidity compared to zeolites. Increasing Al content reduced the order of mesopores. Ideal hydrocracking operation is approached for ASA, MCM-48, and SBA-15 prepared at high pH contained disordered mesopores.	[59]

HYD: Hydrogenation; LHSV: liquid hourly space velocity; TOF: turnover frequency; WHSV: weight hourly space velocity ; 1-MN: 1-methylnaphthalene.

specific products[206,207]. For example, selective coordination and saturation of N-heteroaromatics are important to minimize saturation of unsubstituted aromatics and the need for additional reforming steps to achieve high-octane fuel[119]. There is an increasing need to accommodate feedstocks, such as sour and heavy crudes, bio-oils, waste plastic, biomass, and coal pyrolysis oils, to meet the increasing demand for petroleum products and as alternative sustainable sources, especially biomass and bio-oils. These products come with heavier concentrations of heteroatomic compounds, especially the refractory compounds[7]. They require hydrocracking, yet hydrocracking catalysts are vulnerable to inhibition and poisoning by heteroatoms[207-210]. Considerations for

catalyst deactivation (poisoning by intermediates or products, sintering of support materials or metallic components) and coke deposition need to be made when designing catalysts and choosing operating conditions for these feedstocks[9,209-213]. For example, specific catalysts need to be designed for processing feeds with large concentrations of oxygen-containing compounds since higher amounts of water are produced, which leads to dealumination of alumina supports, and HDO being a highly exothermic process also means increased HDO of higher oxygen content feeds can result in heat build-up in reactors[9,119,211].

The periodic trends for the active metals are well understood, and the high catalytic activities and selectivities of noble metals are not contested. Noble metals are required in small quantities. High HDN activity and HDN/HDS selectivity were obtained through 1% Ir supported on various materials compared to the conventional NiMo system[214]. Nevertheless, the relative abundance of noble metals in the Earth's crust is too low to meet current needs; they are expensive and sensitive to sulfur poisoning[215]. Solutions to increasing the resistance of noble metals to poisoning by sulfur have been explored[52]. They are usually employed as second-stage catalysts in pre-treated feeds that have reduced sulfur[38]. They are useful in shaping the finer properties of oils, e.g., deep desulfurization and hydrogenation. The relative abundance of the non-noble metals that are most active is also much lower than that of the less active ones. Although Mo and W lie in the sweet spot, their abundance is also low and cannot be projected to meet the increasing demand[37,107]. The drive to use other metals, such as Nb, V, and Fe, recently attracted extensive attention, especially iron (Fe). Fe is one of the metals of interest to be considered for substituting the conventionally used catalysts due to its high crust abundance, low cost, and environmental non-toxicity[37,107]. A synergistic effect between Fe and Mo, Ni, or V has been studied for HDS[207]. Although it has been widely considered that the Fe-based catalysts exhibit poor HDS performance, the addition of Zn was found to significantly enhance HDS activity[216]. The promotional effect of Zn comes from the formation of an active FeZnS phase that triggers a strong electron-donating effect from Zn to Fe species and the generation of more sulfur vacancies that change the electronic state of Fe[37,63]. Sudhakar *et al.* patented Fe-Mo sulfide catalysts that are as highly active for HDN as they are for HDS[22]. HDO using Ni-Fe and Ni-Cu has been reported[148,162].

Several efforts are also being made to migrate from traditional sulfides. Various transition metal carbides, nitrides, phosphides, borides, hydrides, oxycarbides, and oxynitrides have been notably tested to modulate the characters of transition metals and obtain noble metal-like properties and even obtain bifunctionality in processes such as hydrocracking[93]. Good HDS and HDN activities have been reported through transition metal carbides[15]. Ternary catalysts for HDS, HDO, HDN, and HDC have also been explored[97]. The metal ratios in the ternary catalysts were found to be important for the concentrations of active phases, dispersion of active phases, and the textural characteristics that influence accessibility of reactive surfaces[121].

Aside from the active metal phase, the catalytic support also has a great influence on the performance of hydroprocessing catalysts[37,63]. The role played by supports is now understood, and modification of supports is now considered a crucial component to achieving high catalyst activity and selectivity. Alumina supports are the most prominent in hydroprocessing catalysts. Their functionality in certain processes is limited due to their strong interaction with the active metals, which impedes sulfidation, resulting in poor catalytic activity. The strong acid sites also promote undesirable reactions that lead to higher coke formation and catalyst deactivation[51,217]. There are various reports on modification of the alumina supports to control the acidity, completely migrating to other support materials such as zeolites or making composite materials to benefit from the attractive properties of multiple support materials[36,76]. For example, chelating agents are used to cover the surface of Al_2O_3 with a carbon layer to reduce the metal support interaction and improve resistance to deactivation by coke deposition. Al_2O_3-carbon composites combine the positive characteristics of the individual components to give optimum support. Mendes *et al.* investigated a Ni_2P catalyst supported

by an Al_2O_3-carbon composite and reported reduced interactions of phosphorus with alumina and minimal formation of inactive P deficient phases, $Ni_{12}P_5$ and $AlPO_4$[215]. The biggest challenge observed when making support material composites was the difficulty in controlling the composition and distribution of mesopores and micropores, which, in turn, affects accessibility and effective promotion of the active metals. The methods used for support preparation are also crucial to get the right catalyst properties such as optimum acidic nature, selectivity, optimal metal-support interaction, and textural properties[35]. The effect of impurities in catalysts also needs to be taken into consideration, and the choice of starting material can be of importance in that regard, as observed in a study where the influence of the Ir precursor: [$Ir(AcAc)_3$, $Ir_4(CO)_{12}$, H_2IrCl_6, $(NH_4)_2IrCl_6$] in obtaining alumina-supported 1% Ir catalysts was investigated and $Ir_4(CO)_{12}$ was found to provide a catalyst with the highest activity owing to less impurities rather than better dispersion of Ir in the catalyst[214].

Overall, multiple factors work in synergy to provide the optimum catalyst performance with suitable properties that allow for a long catalyst lifespan. A balance needs to be struck depending on the feedstocks or expected products.

CONCLUSIONS AND OUTLOOKS

Heterogeneous hydroprocessing catalysis relies on various mineral materials. Wide strides have been made in improving the catalysts following a better understanding of the interactions between the various mineral materials used as supports, active metals, promoters, additives, *etc*. The attractive properties of noble metals (e.g., high activities and selectivities) are identified throughout all the processes discussed in contrast to their vulnerability to poisoning under hydroprocessing conditions (e.g., where sulfur is present) and the fact that they are expensive and found in small quantities. Catalysts with properties that resemble those of noble metal catalysts have been obtained through well-thought combinations of cheaper mineral materials (active and promoter metals and supports), using suitable precursor mineral materials, and understanding synthesis protocols and modifications. Perfecting the catalytic properties using abundant metals such as iron will ensure sustainability, benefitting the hydroprocessing industry and environment in many regards. Better catalysts will also enable the utilization of unconventional feedstocks to meet the increasing demand for particular petroleum products. The review shows that there is a large pool of literature to be repurposed to advance commercialization of technologies involving unconventional feedstocks such as pyrolysis oils, bitumen, and shale-derived oils.

DECLARATIONS

Acknowledgments

We are grateful to Nelson Mandela University for providing the facilities for us to carry out the research.

Authors' contributions

Data curation, interpretation, writing, and editing: Majodina S, Poswayo O, Dembaremba TO
Conception, administrative, technical, material support, and editing: Tshentu ZR

Availability of data and materials

Not applicable.

Financial support and sponsorship

This work was supported by NRF-Sasol Grant (UID138605).

Conflicts of interest

All authors declared that there are no conflicts of interest.

Ethical approval and consent to participate

Not applicable.

Consent for publication

Not applicable.

Copyright

REFERENCES

1. Elnabawy AO, Rangarajan S, Mavrikakis M. Computational chemistry for NH_3 synthesis, hydrotreating, and NO*x* reduction: three topics of special interest to Haldor Topsøe. *J Catal* 2015;328:26-35. DOI
2. Global $9.5 billion refinery catalyst market to 2027 by materials (zeolitea, metallic, chemical compounds), & application (FCC, alkylation, hydrotreating, hydrocracking). Available from: https://www.globenewswire.com/fr/news-release/2021/02/16/2175904/28124/en/Global-9-5-Billion-Refinery-Catalyst-Market-to-2027-by-Material-Zeolites-Metallic-Chemical-Compounds-Application-FCC-Alkylation-Hydrotreating-Hydrocracking.html. [Last accessed on 25 Oct 2023].
3. Afanasiev P, Cattenot M, Geantet C, Matsubayashi N, Sato K, Shimada S. (Ni)W/ZrO_2 hydrotreating catalysts prepared in molten salts. *Appl Catal A Gen* 2002;237:227-37. DOI
4. Hirschon AS, Wilson RB, Laine RM. Ruthenium promoted hydrodenitrogenation catalysts. *Appl Catal* 1987;34:311-6. DOI
5. Addressing sustainability challenges with earth abundant metal catalysis. Available from: https://www.acs.org/acs-webinars/library/abundant-metal-catalysis.html#. [Last accessed on 25 Oct 2023].
6. Sakata Y, Hamrinjr C. Catalytic activity of mineral matter from western Kentucky coals for hydro-desulphurization and hydrodenitrogenation. *Fuel* 1983;62:508-17. DOI
7. Mochida I, Choi K. An overview of hydrodesulfurization and hydrodenitrogenation. *J Jpn Petrol Inst* 2004;47:145-63. DOI
8. Peeters E, Geantet C, Zotin JL, Breysse M, Vrinat M. Deep hydrodenitrogenation on Pt supported catalysts in the presence of H_2S, comparison with NiMo sulfide catalyst. *Stud Surf Sci Catal* 2000;130:2837-42. DOI
9. Robinson PR. 10 - Hydroconversion processes and technology for clean fuel and chemical production. In: Advances in clean hydrocarbon fuel processing. Woodhead Publishing; 2011. p. 287-325. DOI
10. Nagai M, Masunaga T, Hana-oka N. Selectivity of molybdenum catalyst in hydrodenitrogenation, hydrodesulfurization and hydrodeoxygenation: effects of sulfur and oxygen compounds on acridine hydrodenitrogenation. *J Catal* 1986;101:284-92. DOI
11. Katzer JR, Sivasubramanian R. Process and catalyst needs for hydrodenitrogenation. *Catal Rev* 1979;20:155-208. DOI
12. Peeters E, Zotin JL, Geantet C, Breysse M, Vrinat M. Hydrodenitrogenation properties of supported metal catalysts in the presence of H_2S. *Stud Surf Sci Catal* 1999;127:227-34. DOI
13. Oyama ST, Gott T, Zhao H, Lee YK. Transition metal phosphide hydroprocessing catalysts: a review. *Catal Today* 2009;143:94-107. DOI
14. Ho TC. Hydrodenitrogenation catalysis. *Catal Rev* 1988;30:117-60. DOI
15. Lewandowski M, Da Costa P, Benichou D, Sayag C. Catalytic performance of platinum doped tungsten carbide in simultaneous hydrodenitrogenation and hydrodesulphurization. *Appl Catal B Environ* 2010;93:241-9. DOI
16. Yin L, Ma J, Ling L, et al. Insight into the hydrodenitrogenation mechanism of quinoline on the MoP(010) surface with and without the effect of sulfur. *Mol Catal* 2023;538:112970. DOI
17. Farag H. Hydrodesulfurization of dibenzothiophene and 4,6-dimethyldibenzothiophene over NiMo and CoMo sulfide catalysts: kinetic modeling approach for estimating selectivity. *J Colloid Interface Sci* 2010;348:219-26. DOI PubMed
18. Rabarihoela-rakotovao V, Diehl F, Brunet S. Deep HDS of diesel fuel: inhibiting effect of nitrogen compounds on the transformation of the refractory 4,6-dimethyldibenzothiophene over a NiMoP/Al_2O_3 catalyst. *Catal Lett* 2009;129:50-60. DOI
19. Jiang H, Sun X, Lv hailong, et al. Hydrodenitrogenation kinetics of diesel oil and catalyst stacking simulation. *Energy Fuels* 2021;35:3283-94. DOI
20. Reyes JC, Avalos-borja M, Cordero RL, Agudo AL. Influence of phosphorus on the structure and the hydrodesulphurization and hydrodenitrogenation activity of W/Al_2O_3 catalysts. *Appl Catal A Gen* 1994;120:147-62. DOI
21. Fang M, Tang W, Yu C, et al. Performance of Ni-rich bimetallic phosphides on simultaneous quinoline hydrodenitrogenation and dibenzothiophene hydrodesulfurization. *Fuel Process Technol* 2015;129:236-44. DOI
22. Sudhakar C, Sandford G, Dolfinger F. Method for selective hydrodenitrogenation of raw oils. Available from: https://patentimages.storage.googleapis.com/a6/56/a1/1933ab301c78f1/US5389241.pdf. [Last accessed on 25 Oct 2023].
23. Oyama ST. Novel catalysts for advanced hydroprocessing: transition metal phosphides. *J Catal* 2003;216:343-52. DOI

24. Ma Z, Wei L, Zhou W, et al. Overview of catalyst application in petroleum refinery for biomass catalytic pyrolysis and bio-oil upgrading. *RSC Adv* 2015;5:88287-97. DOI
25. Dembaremba TO, Majodina S, Walmsley RS, Ogunlaja AS, Tshentu ZR. Perspectives on strategies for improving ultra-deep desulfurization of liquid fuels through hydrotreatment: catalyst improvement and feedstock pre-treatment. *Front Chem* 2022;10:807225. DOI PubMed PMC
26. Pecoraro TA, Chianelli RR. Hydrodesulfurization catalysis by transition metal sulfides. *J Catal* 1981;67:430-45. DOI
27. Eijsbouts S, de Beer VHJ, Prins R. Periodic trends in the hydrodenitrogenation activity of carbon-supported transition metal sulfide catalysts. *J Catal* 1988;109:217-20. DOI
28. Eijsbouts S, De Beer VHJ, Prins R. Hydrodenitrogenation of quinoline over carbon-supported transition metal sulfides. *J Catal* 1991;127:619-30. DOI
29. Eijsbouts S, Sudhakar C, De Beer VHJ, Prins R. Hydrodenitrogenation of decahydroquinoline, cyclohexylamine and O-propylaniline over carbon-supported transition metal sulfide catalysts. *J Catal* 1991;127:605-18. DOI
30. Raje AP, Liaw SJ, Srinivasan R, Davis BH. Second row transition metal sulfides for the hydrotreatment of coal-derived naphtha I. Catalyst preparation, characterization and comparison of rate of simultaneous removal of total sulfur, nitrogen and oxygen. *Appl Catal A Gen* 1997;150:297-318. DOI
31. Delmon B. New technical challenges and recent advances in hydrotreatment catalysis. A critical updating review. *Catal Lett* 1993;22:1-32. DOI
32. Kazakova MA, Vatutina YV, Selyutin AG, et al. Design of improved CoMo hydrotreating catalyst via engineering of carbon nanotubes@alumina composite support. *Appl Catal B Environ* 2023;328:122475. DOI
33. Hu D, Li H, Mei J, et al. The effect of chelating agent on hydrodesulfurization reaction of ordered mesoporous alumina supported NiMo catalysts. *Pet Sci* 2022;19:321-8. DOI
34. Huang W, Zhou Y, Wei Q, et al. Synthesis of mesoporous TiO2-Al2O3 composites supported Niw hydrotreating catalysts and their superior catalytic performance 3 for heavy oil hydrodenitrogenation. Available from: https://papers.ssrn.com/sol3/papers.cfm?abstract_id=4004949. [Last accessed on 25 Oct 2023]
35. Stolyarova EA, Danilevich VV, Klimov OV, et al. Comparison of alumina supports and catalytic activity of CoMoP/γ-Al_2O_3 hydrotreating catalysts obtained using flash calcination of gibbsite and precipitation method. *Catal Today* 2020;353:88-98. DOI
36. Liu X, Liu J, Li L, et al. Hydrodesulfurization of dibenzothiophene on TiO_2*x*-modified Fe-based catalysts: electron transfer behavior between TiO_2*x* and Fe species. *ACS Catal* 2020;10:9019-33. DOI
37. Wei W, Zhang X, Liu X, et al. Tuning effect of the zeolite brønsted acidity on the FeZn bimetallic hydrodesulfurization catalyst. *Energy Fuels* 2022;36:527-38. DOI
38. Cui T, Rajendran A, Fan H, Feng J, Li W. Review on hydrodesulfurization over zeolite-based catalysts. *Ind Eng Chem Res* 2021;60:3295-323. DOI
39. Aghamohammadi S, Haghighi M, Maleki M, Rahemi N. Sequential impregnation vs. sol-gel synthesized Ni/Al_2O_3-CeO_2 nanocatalyst for dry reforming of methane: effect of synthesis method and support promotion. *Mol Catal* 2017;431:39-48. DOI
40. Li T, Tao Z, Hu C, et al. Brønsted acidity of amorphous silica-aluminas for hydrocracking of Fischer-Tropsch wax into diesel fractions. *Appl Catal A Gen* 2022;630:118439. DOI
41. Shi G, Fang D, Shen J. Hydroisomerization of model FCC naphtha over sulfided Co(Ni)-Mo(W)/MCM-41 catalysts. *Microporous Mesoporous Mater* 2009;120:339-45. DOI
42. Cao Z, Zhang X, Guo R, et al. Synergistic effect of acidity and active phases for NiMo catalysts on dibenzothiophene hydrodesulfurization performance. *Chem Eng J* 2020;400:125886. DOI
43. Zhou W, Yang L, Liu L, et al. Synthesis of novel NiMo catalysts supported on highly ordered TiO_2-Al_2O_3 composites and their superior catalytic performance for 4,6-dimethyldibenzothiophene hydrodesulfurization. *Appl Catal B Environ* 2020;268:118428. DOI
44. Zhang P, Mu F, Zhou Y, et al. Synthesis of highly ordered TiO_2-Al_2O_3 and catalytic performance of its supported NiMo for HDS of 4, 6-dimethyldibenzothiophene. *Catal Today* 2023;423:112716. DOI
45. Chen J, Xia B, Zheng M, et al. Hydrotreatment of FCC gasoline catalyzed by CoMo bifunctional catalysts: the effects of acidity on catalytic performance. *Ind Eng Chem Res* 2021;60:173-84. DOI
46. Kazakova MA, Vatutina YV, Prosvirin IP, et al. Boosting hydrodesulfurization activity of CoMo/Al_2O_3 catalyst via selective graphitization of alumina surface. *Microporous Mesoporous Mater* 2021;317:111008. DOI
47. Zhang G, Yang F, Xu Z, et al. Electronic structure regulation of CoMoS catalysts by N, P co-doped carbon modification for effective hydrodesulfurization. *Fuel* 2022;322:124160. DOI
48. Saleh TA, Sulaiman KO, Al-hammadi SA. Effect of carbon on the hydrodesulfurization activity of MoCo catalysts supported on zeolite/ active carbon hybrid supports. *Appl Catal B Environ* 2020;263:117661. DOI
49. Kohli K, Prajapati R, Maity SK, Sharma BK. Effect of silica, activated carbon, and alumina supports on NiMo catalysts for residue upgrading. *Energies* 2020;13:4967. DOI
50. Huirache-acuña R, Pérez-ayala E, Cervantes-gaxiola M, et al. Dibenzothiophene hydrodesulfurization over ternary metallic NiMoW/Ti-HMS mesoporous catalysts. *Catal Commun* 2021;148:106162. DOI
51. Roy T, Rousseau J, Daudin A, et al. Deep hydrodesulfurization of 4,6-dimethydibenzothiophene over CoMoS/TiO_2 catalysts: impact of the TiO_2 treatment. *Catal Today* 2021;377:17-25. DOI
52. Yerga RM, Pawelec B, Mota N, Huirache-Acuña R. Hydrodesulfurization of dibenzothiophene over Ni-Mo-W sulfide catalysts

supported on sol-gel Al_2O_3-CeO_2. *Materials* 2022;15:6780. DOI PubMed PMC
53. Duan P, Savage PE. Catalytic hydrothermal hydrodenitrogenation of pyridine. *Appl Catal B Environ* 2011;108-9:54-60. DOI
54. Guo Y, Liu X, Duan P, Xu D, Luque R. Catalytic hydrodenitrogenation of pyridine under hydrothermal conditions: a comprehensive study. *ACS Sustain Chem Eng* 2021;9:362-74. DOI
55. Fisk CA, Morgan T, Ji Y, Crocker M, Crofcheck C, Lewis SA. Bio-oil upgrading over platinum catalysts using *in situ* generated hydrogen. *Appl Catal A Gen* 2009;358:150-6. DOI
56. Ambursa MM, Birnin-Yauri AU, Yahya Y, Wawata IG, Yusuf AB. A review on required catalysts composition and its effective preparation method for hydrodeoxygenation of bio-oil. *Equity J Sci Technol* 2020;7:136-43. Available from: https://www.ajol.info/index.php/equijost/article/view/214425. [Last accessed on 25 Oct 2023]
57. Lebeau B, Bonne M, Comparot JD, et al. HDS of 4,6-dimethyldibenzothiophene over CoMoS supported mesoporous SiO_2-TiO_2 materials. *Catal Today* 2020;357:675-83. DOI
58. Liu C, Mei J, Wang G, et al. Tailoring NiMoS active phases with high hydrodesulfurization activity through facilely synthesized supports with tunable mesostructure and morphology. *J Catal* 2020;387:170-85. DOI
59. Romero DE, Rigutto M, Hensen EJM. Influence of the size, order and topology of mesopores in bifunctional Pd-containing acidic SBA-15 and M41S catalysts for n-hexadecane hydrocracking. *Fuel Process Technol* 2022;232:107259. DOI
60. Keivanimehr F, Habibzadeh S, Mokhtarian M. Enhanced product quality through hydrodesulfurization of pyrolysis gasoline over a mixed metal oxide catalyst: an experimental and DFT study. *Fuel* 2022;317:123458. DOI
61. Zhou W, Liu M, Zhang Q, Wei Q, Ding S, Zhou Y. Synthesis of NiMo catalysts supported on gallium-containing mesoporous Y zeolites with different gallium contents and their high activities in the hydrodesulfurization of 4,6-dimethyldibenzothiophene. *ACS Catal* 2017;7:7665-79. DOI
62. Acosta-silva YJ, Toledano-ayala M, Torres-delgado G, et al. Nanostructured CeO_2 thin films prepared by the sol-gel dip-coating method with anomalous behavior of crystallite size and bandgap. *J Nanomater* 2019;2019:1-8. DOI
63. Liu X, Liu J, Li L, et al. Preparation of electron-rich Fe-based catalyst via electronic structure regulation and its promotion to hydrodesulfurization of dibenzothiophene. *Appl Catal B Environ* 2020;269:118779. DOI
64. Ramírez-lópez R, Elizalde I, Rodríguez-méndez EE, Mera-luna S, Flores-vela AI. Al_2O_3-CeO_2 sol-gel synthesis and addition of Rh to improve the oxygen mobility of mixed support. *J Sol-Gel Sci Technol* 2017;81:214-9. DOI
65. Tai L, Hamidi R, de Caprariis B, et al. Guaiacol hydrotreating with in-situ generated hydrogen over ni/modified zeolite supports. *Renew Energy* 2022;182:647-58. DOI
66. Zhou W, Zhou A, Zhang Y, et al. Hydrodesulfurization of 4,6-dimethyldibenzothiophene over NiMo supported on Ga-modified Y zeolites catalysts. *J Catal* 2019;374:345-59. DOI
67. Ward JW. Hydrocracking processes and catalysts. *Fuel Process Technol* 1993;35:55-85. DOI
68. Vela FJ, Palos R, García JR, et al. Enhancing the performance of a PtPd/HY catalyst for HDPE/VGO hydrocracking through zeolite desilication. *Fuel* 2022;329:125392. DOI
69. Salam MA, Arora P, Ojagh H, Cheah YW, Olsson L, Creaser D. NiMoS on alumina-USY zeolites for hydrotreating lignin dimers: effect of support acidity and cleavage of C-C bonds. *Sustain Energy Fuels* 2020;4:149-63. DOI
70. Jabłońska M, Król A, Kukulska-zając E, et al. Zeolites Y modified with palladium as effective catalysts for low-temperature methanol incineration. *Appl Catal B Environ* 2015;166-7:353-65. DOI
71. Silva B, Figueiredo H, Soares O, et al. Evaluation of ion exchange-modified Y and ZSM5 zeolites in Cr(VI) biosorption and catalytic oxidation of ethyl acetate. *Appl Catal B Environ* 2012;117-8:406-13. DOI
72. Ma J, Kang Y, Ma N, Hao W, Wang Y, Li R. A high acid mesoporous USY zeolite prepared by alumination. *Mater Sci Pol* 2013;31:19-24. DOI
73. Lin TJ, Meng X, Shi L. Ni-exchanged Y-zeolite: An efficient heterogeneous catalyst for acetylene hydrocarboxylation. *Appl Catal A Gen* 2014;485:163-71. DOI
74. Agudelo JL, Hensen EJM, Giraldo SA, Hoyos LJ. Effect of USY zeolite chemical treatment with ammonium nitrate on its VGO hydrocracking performance. *Energy Fuels* 2016;30:616-25. DOI
75. Zepeda TA, Pawelec B, Díaz de León JN, de los Reyes JA, Olivas A. Effect of gallium loading on the hydrodesulfurization activity of unsupported Ga2S3/WS2 catalysts. *Appl Catal B Environ* 2012;111-2:10-9. DOI
76. Vitolo S, Seggiani M, Frediani P, Ambrosini G, Politi L. Catalytic upgrading of pyrolytic oils to fuel over different zeolites. *Fuel* 1999;78:1147-59. DOI
77. Saab R, Polychronopoulou K, Anjum DH, et al. Effect of SiO_2/Al_2O_3 ratio in Ni/Zeolite-Y and Ni-W/Zeolite-Y catalysts on hydrocracking of heptane. *Mol Catal* 2022;528:112484. DOI
78. Mendes F, Teixeira da Silva V, Edral Pacheco M, de Rezende Pinho A, Assumpção Henriques C. Hydrotreating of fast pyrolysis oil: a comparison of carbons and carbon-covered alumina as supports for Ni_2P. *Fuel* 2020;264:116764. DOI
79. Kazakov M, Kazakova M, Vatutina Y, et al. Comparative study of MWCNT and alumina supported CoMo hydrotreating catalysts prepared with citric acid as chelating agent. *Catal Today* 2020;357:221-30. DOI
80. Xu Z, Wang H, Kang H, et al. Effect of organic phosphorus addition on the state of active metal species and catalytic performance of NiW/Al_2O_3 hydrodesulfurization catalyst. *Fuel* 2023;340:127547. DOI
81. Huang W, Wei Q, Zhou Y, et al. Hydrotreating of diesel fuel over in-situ nickel modified Y zeolite supported Ni-Mo-S catalyst. *Catal Today* 2023;407:135-45. DOI

82. Ali I, Al-shafei EN, Al-arfaj AA, Saleh TA. Influence of titanium oxide on the performance of molybdenum catalysts loaded on zeolite toward hydrodesulfurization reactions. *Microporous Mesoporous Mater* 2020;303:110188. DOI
83. Cao Z, Guo R, Du P, et al. Synthesis of highly ordered Al-Zr-SBA-16 composites and their application in dibenzothiophene hydrodesulfurization. *Chem Eng Sci* 2020;213:115415. DOI
84. Zhang B, Seddon D. Hydroprocessing catalysts and processes: the challenges for biofuels production. In: Catalytic science series. Europe: World Scientific; 2018. p. 316. DOI
85. Xia B, Cao L, Luo K, et al. Effects of the active phase of CoMo/γ-Al_2O_3 catalysts modified using cerium and phosphorus on the HDS performance for FCC gasoline. *Energy Fuels* 2019;33:4462-73. DOI
86. He S, Huang T, Fan Y. Tetradecylamine-induced assembly of Mo and Al precursors to prepare efficient NiMoS/Al_2O_3 catalysts for ultradeep hydrodesulfurization. *Appl Catal B Environ* 2022;317:121801. DOI
87. Rayo P, Torres-mancera P, Centeno G, Alonso F, Muñoz JAD, Ancheyta J. Effect of silicon incorporation method in the supports of NiMo catalysts for hydrotreating reactions. *Fuel* 2019;239:1293-303. DOI
88. Wang G, Zhao Z, Zhou W, et al. Investigation on the mechanism of 4,6-dimenthyldibenzothiophehe over NiMoS catalyst supported on highly ordered TiO2-Al2O3 composites-role of the solvent evaporating temperature. Available from: https://papers.ssrn.com/sol3/papers.cfm?abstract_id=4069628. [Last accessed on 25 Oct 2023].
89. Danilova IG, Dik PP, Sorokina TP, et al. Effect of rare earths on acidity of high-silica ultrastable REY zeolites and catalytic performance of NiMo/REY+Al_2O_3 catalysts in vacuum gas oil hydrocracking. *Microporous Mesoporous Mater* 2022;329:111547. DOI
90. Qu L. Support and fluorination effects in hydrodenitrogenation over Ni-Mo hydrotreating catalysts. Available from: https://www.research-collection.ethz.ch/bitstream/handle/20.500.11850/146933/eth-25898-02.pdf. [Last accessed on 25 Oct 2023].
91. Yan P, Tao Z, Hao K, Wang Y, Yang Y, Li Y. Effect of impregnation methods on nickel-tungsten catalysts and its performance on hydrocracking Fischer-Tropsch wax. *J Fuel Chem Technol* 2013;41:691-7. DOI
92. Nikulshina M, Kokliukhin A, Mozhaev A, Nikulshin P. CoMo/Al_2O_3 hydrotreating catalysts prepared from single Co_2Mo_{10}-heteropolyacid at extremely high metal loading. *Catal Commun* 2019;127:51-7. DOI
93. Prins R. Catalytic hydrodenitrogenation. *Adv Catal* 2001;46:399-464. DOI
94. Vázquez-garrido I, López-benítez A, Berhault G, Guevara-lara A. Effect of support on the acidity of NiMo/Al_2O_3-MgO and NiMo/TiO_2-Al_2O_3 catalysts and on the resulting competitive hydrodesulfurization/hydrodenitrogenation reactions. *Fuel* 2019;236:55-64. DOI
95. Zhang L, Chen X, Chen Y, Li W, Yang K, Liang C. Non-metal doping Ni@C as highly efficient and stable hydrodesulfurization catalysts for clean liquid fuels. *Mol Catal* 2022;528:112440. DOI
96. Zhang S, Nguyen L, Liang JX, et al. Catalysis on singly dispersed bimetallic sites. *Nat Commun* 2015;6:7938. DOI
97. Topalian PJ, Carrillo BA, Cochran PM, Takemura MF, Bussell ME. Synthesis and hydrodesulfurization properties of silica-supported nickel-ruthenium phosphide catalysts. *J Catal* 2021;403:173-80. DOI
98. Yue S, Xu D, Sheng Y, et al. One-step synthesis of mesoporous alumina-supported molybdenum carbide with enhanced activity for thiophene hydrodesulfurization. *J Environ Cheml Eng* 2021;9:105693. DOI
99. Lin Z, Denny SR, Chen JG. Transition metal carbides and nitrides as catalysts for thermochemical reactions. *J Catal* 2021;404:929-42. DOI
100. Shamanaev IV, Suvorova AO, Gerasimov EY, et al. SRGO hydrotreating over Ni-phosphide catalysts on granulated Al_2O_3. *Catal Today* 2021;378:24-32. DOI
101. Cecilia J, Infantes-molina A, Rodríguez-castellón E, Jiménez-lópez A. A novel method for preparing an active nickel phosphide catalyst for HDS of dibenzothiophene. *J Catal* 2009;263:4-15. DOI
102. Wang C, Li X, Liu Y, Wang A, Sheng Q, Zhang C. Insight into metal-support interactions from the hydrodesulfurization of dibenzothiophene over Pd catalysts supported on UiO-66 and its amino-functionalized analogues. *J Catal* 2022;407:333-41. DOI
103. Dai X, Cheng Y, Si M, et al. A non-noble metal supported catalyst with potential prospect for hydroisomerization of n-hexadecane: second metal incorporated NiMe/SAPO-11 catalyst with superior hydroisomerization performance. *Fuel* 2022;324:124517. DOI
104. Weise CF, Falsig H, Moses PG, Helveg S, Brorson M, Hansen LP. Single-atom Pt promotion of industrial Co-Mo-S catalysts for ultra-deep hydrodesulfurization. *J Catal* 2021;403:74-86. DOI
105. Majodina S, Tshentu ZR, Ogunlaja AS. Effect of adding chelating ligands on the catalytic performance of Rh-promoted MoS_2 in the hydrodesulfurization of dibenzothiophene. *Catalysts* 2021;11:1398. DOI
106. Dong C, Yin C, Wu T, Wu Z, Liu D, Liu C. Effect of β-zeolite nanoclusters on the acidity and hydrodesulfurization activity of an unsupported Ni Mo catalyst. *Catal Commun* 2019;119:164-9. DOI
107. Li L, Wang M, Huang L, et al. Electron-donating-accepting behavior between nitrogen-doped carbon materials and Fe species and its promotion for DBT hydrodesulfurization. *Appl Catal B Environ* 2019;254:360-70. DOI
108. Farag H, Kishida M, Al-megren H. Competitive hydrodesulfurization of dibenzothiophene and hydrodenitrogenation of quinoline over unsupported MoS_2 catalyst. *Appl Catal A General* 2014;469:173-82. DOI
109. Castillo-Villalón P, Ramírez J, Reyes-sosa A, et al. On the contribution of the cobalt sulfide phase to the global activity of industrial-type CoMo/Al_2O_3 catalysts in the HDS of DBT. *Catal Today* 2022;394-6:41-9. DOI
110. Qi L, Zheng P, Zhao Z, Duan A, Xu C, Wang X. Insights into the intrinsic kinetics for efficient hydrodesulfurization of 4,6-dimethyldibenzothiophene over mesoporous $CoMoS_2$/ZSM-5. *J Catal* 2022;408:279-93. DOI

111. Chen Z, Liu Y, Chen J, et al. Synthesis of alumina-nitrogen-doped carbon support for CoMo catalysts in hydrodesulfurization process. *Chin J Chem Eng* 2022;41:392-402. DOI
112. Egorova M, Prins R. Competitive hydrodesulfurization of 4,6-dimethyldibenzothiophene, hydrodenitrogenation of 2-methylpyridine, and hydrogenation of naphthalene over sulfided NiMo/γ-Al_2O_3. *J Catal* 2004;224:278-87. DOI
113. Chowdari RK, Díaz de León JN, Fuentes-moyado S. Effect of sulfidation conditions on the unsupported flower-like bimetallic oxide microspheres for the hydrodesulfurization of dibenzothiophene. *Catal Today* 2022;394-6:13-24. DOI
114. Rajendran A, Cui TY, Fan HX, Wang MY, Li WY. High-performance NiMoS hydrodesulfurization catalysts by one-pot hydrothermal synthesis using $Ni(acac)_2$ for sulfur-free liquid fuels. *Fuel Process Technol* 2022;227:107101. DOI
115. Kanda Y, Saito R, Ono T, et al. Enhancement of the hydrodesulfurization and C-S bond cleavage activities of rhodium phosphide catalysts by platinum addition. *J Catal* 2022;408:294-302. DOI
116. Prado GHC, Rao Y, de Klerk A. Nitrogen removal from oil: a review. *Energy Fuels* 2017;31:14-36. DOI
117. Prins R, Zhao Y, Sivasankar N, Kukula P. Mechanism of C-N bond breaking in hydrodenitrogenation. *J Catal* 2005;234:509-12. DOI
118. Sinfelt JH. Chemistry of catalytic processes, by Bruce C. Gates, James R. Katzer, and G. C. A. Schuit. Mcgraw-Hill, 1979, 464 pp. $28.50. *AIChE J* 1979;25:734. DOI
119. Bachrach M, Marks TJ, Notestein JM. Understanding the hydrodenitrogenation of heteroaromatics on a molecular level. *ACS Catal* 2016;6:1455-76. DOI
120. Peeters E, Cattenot M, Geantet C, Breysse M, Zotin JL. Hydrodenitrogenation on Pt/silica-alumina catalysts in the presence of H_2S: role of acidity. *Catal Today* 2008;133-5:299-304. DOI
121. Albersberger S, Shi H, Wagenhofer M, Han J, Gutiérrez OY, Lercher JA. On the enhanced catalytic activity of acid-treated, trimetallic Ni-Mo-W sulfides for quinoline hydrodenitrogenation. *J Catal* 2019;380:332-42. DOI
122. Joo H, Guin JA. Activity of noble metal-promoted hydroprocessing catalysts for pyridine HDN and naphthalene hydrogenation. *Fuel Process Technol* 1996;49:137-55. DOI
123. Li S, Sung Lee J, Hyeon T, Suslick KS. Catalytic hydrodenitrogenation of indole over molybdenum nitride and carbides with different structures. *Appl Catal A Gen* 1999;184:1-9. DOI
124. Al-megren HA, Xiao T, Gonzalez-cortes SL, Al-khowaiter SH, Green ML. Comparison of bulk CoMo bimetallic carbide, oxide, nitride and sulfide catalysts for pyridine hydrodenitrogenation. *J Mol Catal A Chem* 2005;225:143-8. DOI
125. Miga K, Stanczyk K, Sayag C, Brodzki D, Djéga-mariadassou G. Bifunctional behavior of bulk MoOxNyand nitrided supported NiMo catalyst in hydrodenitrogenation of indole. *J Catal* 1999;183:63-8. DOI
126. Qiu Z, Wang Y, Li Z, Cao Y, Li Q. Hydrodenitrogenation of Quinoline with high selectivity to aromatics over α-MoC1-x. *Mol Catal* 2021;516:112002. DOI
127. Zuzaniuk V, Prins R. Synthesis and characterization of silica-supported transition-metal phosphides as HDN catalysts. *J Catal* 2003;219:85-96. DOI
128. Wagner JL, Jones E, Sartbaeva A, et al. Zeolite Y supported nickel phosphide catalysts for the hydrodenitrogenation of quinoline as a proxy for crude bio-oils from hydrothermal liquefaction of microalgae. *Dalton Trans* 2018;47:1189-201. DOI
129. Lewandowski M. Hydrotreating activity of bulk NiB alloy in model reaction of hydrodenitrogenation of carbazole. *Appl Catal B Environ* 2015;168-9:322-32. DOI
130. Clark P, Dhandapani B, Oyama ST. Preparation and hydrodenitrogenation performance of rhenium nitride. *Appl Catal A Gen* ;184:175-80. DOI
131. Choi JG, Brenner JR, Colling CW, Demczyk BG, Dunning JL, Thompson LT. Synthesis and characterization of molybdenum nitride hydrodenitrogenation catalysts. *Catal Today* 1992;15:201-22. DOI
132. Lee KS, Reimer JA, Bell AT. Investigations of hydrodenitrogenation of quinoline over molybdenum nitride. *Stud Surf Sci Catal* 1993;75:2197-200. DOI
133. Delmon B, Grange P, Froment GF. Hydrotreatment and hydrocracking of oil fractions. Available from: https://shop.elsevier.com/books/hydrotreatment-and-hydrocracking-of-oil-fractions/delmon/978-0-444-82556-8. [Last accessed on 25 Oct 2023].
134. Ledesma BC, Martínez ML, Beltramone AR. Iridium-supported SBA-15 modified with Ga and Al as a highly active catalyst in the hydrodenitrogenation of quinoline. *Catal Today* 2020;349:178-90. DOI
135. Escalona N, Vrinat M, Laurenti D, Gil Llambías F. Rhenium sulfide in hydrotreating. *Appl Catal A Gen* 2007;322:113-20. DOI
136. Luchsinger M, Bozkurt B, Akgerman A, Janzen C, Addiego W, Darensbourg M. Direct synthesis of mixed metal sulfide catalysts and their hydrodenitrogenation activity. *Appl Catal* 1991;68:229-47. DOI
137. Klimov OV, Nadeina KA, Vatutina YV, et al. CoMo/Al_2O_3 hydrotreating catalysts of diesel fuel with improved hydrodenitrogenation activity. *Catal Today* 2018;307:73-83. DOI
138. Nagai M, Goto Y, Irisawa A, Omi S. Catalytic activity and surface properties of nitrided molybdena-alumina for carbazole hydrodenitrogenation. *J Catal* 2000;191:128-37. DOI
139. Szymańska A, Lewandowski M, Sayag C, Djéga-Mariadassou G. Kinetic study of the hydrodenitrogenation of carbazole overbulkmolybdenum carbide. *J Catal* 2003;218:24-31. DOI
140. Szymańska-kolasa A, Lewandowski M, Sayag C, Brodzki D, Djéga-mariadassou G. Comparison between tungsten carbide and molybdenum carbide for the hydrodenitrogenation of carbazole. *Catal Today* 2007;119:35-8. DOI
141. Bowker RH, Ilic B, Carrillo BA, Reynolds MA, Murray BD, Bussell ME. Carbazole hydrodenitrogenation over nickel phosphide and Ni-rich bimetallic phosphide catalysts. *Appl Catal A Gen* 2014;482:221-30. DOI
142. Stinner C, Prins R, Weber T. Binary and ternary transition-metal phosphides as HDN catalysts. *J Catal* 2001;202:187-94. DOI

143. de Souza Guedes Junior G, Gigante Nascimento I, Ahmad M, et al. Kinetics of simultaneous hydrodesulfurization and hydrodenitrogenation reactions using CoMoP/Al_2O_3 and NiMoP/Al_2O_3. *Chem Eng Sci* 2023;275:118725. DOI
144. Wang J, Wang X, Yuan Y, Shuaib A, Shen J. Optimization of MgO/Al_2O_3 ratio for the maximization of active site densities in the Ni_2P/MgAlO catalysts for the hydrotreating reactions. *J Energy Chem* 2016;25:571-6. DOI
145. Sureshkumar K, Shanthi K, Sasirekha N, Jegan J, Sardhar Basha S. A study on catalytic activity of modified Ni-Re/Al-SBA-15 catalyst for hydrodenitrogenation of o-toluidine. *Int J Hydrog Energy* 2020;45:4328-40. DOI
146. Cinibulk J, Vít Z. Selective Mo-Ir/Al_2O_3 sulfide catalysts for hydrodenitrogenation. *Appl Catal A Gen* 2000;204:107-16. DOI
147. Wandas R, Surygala J, Śliwka E. Conversion of cresols and naphthalene in the hydroprocessing of three-component model mixtures simulating fast pyrolysis tars. *Fuel* 1996;75:687-94. DOI
148. Leng S, Wang X, He X, et al. NiFe/γ-Al_2O_3: a universal catalyst for the hydrodeoxygenation of bio-oil and its model compounds. *Catal Commun* 2013;41:34-7. DOI
149. Zhang Z, Pei Z, Chen H, et al. Catalytic in-situ hydrogenation of furfural over bimetallic Cu-Ni alloy catalysts in isopropanol. *Ind Eng Chem Res* 2018;57:4225-30. DOI
150. Xue H, Xu J, Gong X, Hu R. Performance of a Ni-Cu-Co/Al_2O_3 catalyst on in-situ hydrodeoxygenation of bio-derived phenol. *Catalysts* 2019;9:952. DOI
151. Toba M, Abe Y, Kuramochi H, Osako M, Mochizuki T, Yoshimura Y. Hydrodeoxygenation of waste vegetable oil over sulfide catalysts. *Catal Today* 2011;164:533-7. DOI
152. Massoth FE, Politzer P, Concha MC, Murray JS, Jakowski J, Simons J. Catalytic hydrodeoxygenation of methyl-substituted phenols: correlations of kinetic parameters with molecular properties. *J Phys Chem B* 2006;110:14283-91. DOI PubMed
153. Priecel P, Kubička D, Čapek L, Bastl Z, Ryšánek P. The role of Ni species in the deoxygenation of rapeseed oil over NiMo-alumina catalysts. *Appl Catal A Gen* 2011;397:127-37. DOI
154. Kubička D, Kaluža L. Deoxygenation of vegetable oils over sulfided Ni, Mo and NiMo catalysts. *Appl Catal A Gen* 2010;372:199-208. DOI
155. Kimura T, Imai H, Li X, Sakashita K, Asaoka S, Al-khattaf SS. Hydroconversion of triglycerides to hydrocarbons over Mo-Ni/γ-Al_2O_3 catalyst under low hydrogen pressure. *Catal Lett* 2013;143:1175-81. DOI
156. Hachemi I, Jeništová K, Mäki-arvela P, et al. Comparative study of sulfur-free nickel and palladium catalysts in hydrodeoxygenation of different fatty acid feedstocks for production of biofuels. *Catal Sci Technol* 2016;6:1476-87. DOI
157. Popov A, Kondratieva E, Mariey L, et al. Bio-oil hydrodeoxygenation: adsorption of phenolic compounds on sulfided (Co)Mo catalysts. *J Catal* 2013;297:176-86. DOI
158. Centeno A, Laurent E, Delmon B. Influence of the support of CoMo sulfide catalysts and of the addition of potassium and platinum on the catalytic performances for the hydrodeoxygenation of carbonyl, carboxyl, and guaiacol-type molecules. *J Catal* 1995;154:288-98. DOI
159. Şenol OI, Viljava TR, Krause AOI. Hydrodeoxygenation of methyl esters on sulphided NiMo/γ-Al_2O_3 and CoMo/γ-Al_2O_3 catalysts. *Catal Today* 2005;100:331-5. DOI
160. Tiwari R, Rana BS, Kumar R, et al. Hydrotreating and hydrocracking catalysts for processing of waste soya-oil and refinery-oil mixtures. *Catal Commun* 2011;12:559-62. DOI
161. Li X, Luo X, Jin Y, et al. Heterogeneous sulfur-free hydrodeoxygenation catalysts for selectively upgrading the renewable bio-oils to second generation biofuels. *Renew Sustain Energy Rev* 2018;82:3762-97. DOI
162. Ardiyanti AR, Khromova SA, Venderbosch RH, Yakovlev VA, Heeres HJ. Catalytic hydrotreatment of fast-pyrolysis oil using non-sulfided bimetallic Ni-Cu catalysts on a δ-Al_2O_3 support. *Appl Catal B Environ* 2012;117-8:105-17. DOI
163. Horáček J, Tišler Z, Rubáš V, Kubička D. HDO catalysts for triglycerides conversion into pyrolysis and isomerization feedstock. *Fuel* 2014;121:57-64. DOI
164. la Puente G, Gil A, Pis JJ, Grange P. Effects of support surface chemistry in hydrodeoxygenation reactions over CoMo/activated carbon sulfided catalysts. *Langmuir* 1999;15:5800-6. DOI
165. Yang Y, Gilbert A, Xu C(C). Hydrodeoxygenation of bio-crude in supercritical hexane with sulfided CoMo and CoMoP catalysts supported on MgO: a model compound study using phenol. *Appl Catal A Gen* 2009;360:242-9. DOI
166. Echeandia S, Arias P, Barrio V, Pawelec B, Fierro J. Synergy effect in the HDO of phenol over Ni-W catalysts supported on active carbon: effect of tungsten precursors. *Appl Catal B Environ* 2010;101:1-12. DOI
167. Yoosuk B, Tumnantong D, Prasassarakich P. Amorphous unsupported Ni-Mo sulfide prepared by one step hydrothermal method for phenol hydrodeoxygenation. *Fuel* 2012;91:246-52. DOI
168. Zhang D, Ye F, Xue T, Guan Y, Wang YM. Transfer hydrogenation of phenol on supported Pd catalysts using formic acid as an alternative hydrogen source. *Catal Today* 2014;234:133-8. DOI
169. Xiang Y, Li X, Lu C, Ma L, Yuan J, Feng F. Reaction performance of hydrogen from aqueous-phase reforming of methanol or ethanol in hydrogenation of phenol. *Ind Eng Chem Res* 2011;50:3139-44. DOI
170. Snåre M, Kubičková I, Mäki-arvela P, Eränen K, Murzin DY. Heterogeneous catalytic deoxygenation of stearic acid for production of biodiesel. *Ind Eng Chem Res* 2006;45:5708-15. DOI
171. Wildschut J, Mahfud FH, Venderbosch RH, Heeres HJ. Hydrotreatment of fast pyrolysis oil using heterogeneous noble-metal catalysts. *Ind Eng Chem Res* 2009;48:10324-34. DOI
172. Zhao X, Cai Z, Wang T, O'reilly S, Liu W, Zhao D. A new type of cobalt-deposited titanate nanotubes for enhanced photocatalytic

degradation of phenanthrene. *Appl Catal B Environ* 2016;187:134-43. DOI

173. Ghassabzadeh H, Rashidzadeh M, Niaei A. A novel fast evaluation method for mesoporous NiMo/Al_2O_3 hydrodemetallization (HDM) catalysts: activity and metal uptake capacity measurements. *Reac Kinet Mech Cat* 2020;130:381-402. DOI
174. Sui B, Wang G, Yuan S, et al. Macroporous Al_2O_3 with three-dimensionally interconnected structure: catalytic performance of hydrodemetallization for residue oil. *J Fuel Chem Technol* 2021;49:1201-7. DOI
175. Kim J, Longstaff DC, Hanson FV. Upgrading of bitumen-derived heavy oils over a commercial HDN catalyst. *Fuel* 1997;76:1143-50. DOI
176. Ancheyta-juárez J, Maity S, Betancourt-rivera G, Centeno-nolasco G, Rayo-mayoral P, Gómez-pérez M. Comparison of different Ni-Mo/alumina catalysts on hydrodemetallization of Maya crude oil. *Appl Catal A Gen* 2001;216:195-208. DOI
177. Liu T, Ju L, Zhou Y, et al. Effect of pore size distribution (PSD) of Ni-Mo/Al_2O_3 catalysts on the Saudi Arabia vacuum residuum hydrodemetallization (HDM). *Catal Today* 2016;271:179-87. DOI
178. Rana MS, Alhumaidan FS, Navvamani R. Synthesis of large pore carbon-alumina supported catalysts for hydrodemetallization. *Catal Today* 2020;353:204-12. DOI
179. Zhang B. Chapter 1: Hydroprocessing and the chemistry. In: Hydroprocessing catalysts and processes. Europe: World Scientific; 2018. p. 1-56. DOI
180. Shi Y, Yang C, Zhao X, et al. Engineering the hierarchical pore structures and geometries of hydrodemetallization catalyst pellets. *Ind Eng Chem Res* 2019;58:9829-37. DOI
181. Garcia-Montoto V, Verdier S, Maroun Z, et al. Understanding the removal of V, Ni and S in crude oil atmospheric residue hydrodemetallization and hydrodesulfurization. *Fuel Process Technol* 2020;201:106341. DOI
182. León AY, Guzman A, Laverde D, Chaudhari RV, Subramaniam B, Bravo-suárez JJ. Thermal cracking and catalytic hydrocracking of a colombian vacuum residue and its maltenes and asphaltenes fractions in toluene. *Energy Fuels* 2017;31:3868-77. DOI
183. Rana MS, Ancheyta J, Maity S, Rayo P. Maya crude hydrodemetallization and hydrodesulfurization catalysts: an effect of TiO_2 incorporation in Al_2O_3. *Catal Today* 2005;109:61-8. DOI
184. Rana MS, Alhumaidan FS. Hydrometallization catalysts. Available from: https://patents.google.com/patent/US9861972B1/en. [Last accessed on 25 Oct 2023].
185. Dillon CJ, Maesen T, Kuperman AE. Hydrometallization catalyst and process. Available from: https://patents.google.com/patent/US8716164B2/en. [Last accessed on 25 Oct 2023].
186. Liu Z, Yuan J, Sun Z, et al. Morphology effect on catalytic performance of ebullated-bed residue hydrotreating over Ni-Mo/Al_2O_3 catalyst: a kinetic modeling study. *Green Chem Eng* 2022;In press. DOI
187. Ghassabzaadeh H, Niaei A, Rashidzadeh M. Synthesis and characterization of multi-modal γ-Al_2O_3: a systematic investigation on the optimization of hydrodemetallization catalyst preparation. *ChemistrySelect* 2020;5:8892-905. DOI
188. Kirgizov AY, Ding B, Spiridonov AA, et al. Ex situ upgrading of extra heavy oil: the effect of pore shape of Co-Mo/γ-Al_2O_3 catalysts. *Catalysts* 2022;12:1271. DOI
189. Langlois GE, Sullivan RF. Chemistry of hydrocracking. In: Spillane LJ, Leftin HP, editors. Refining petroleum for chemicals. Washington: American Chemical Society; 1970. p. 38-67. DOI
190. Muralidhar G, Massoth FE, Shabtai J. Catalytic functionalities of supported sulfides: I. Effect of support and additives on the CoMo catalyst. *J Catal* 1984;85:44-52. DOI
191. Speight JG, El-Gendy NS. Introduction to petroleum biotechnology. Available from: https://www.sciencedirect.com/book/9780128051511/introduction-to-petroleum-biotechnology?via=ihub=. [Last accessed on 25 Oct 2023].
192. Weitkamp J. Catalytic hydrocracking-mechanisms and versatility of the process. *ChemCatChem* 2012;4:292-306. DOI
193. Choudhary N, Saraf DN. Hydrocracking: a review. *Ind Eng Chem Prod Res Dev* 1975;14:74-83. DOI
194. Mohanty S, Kunzru D, Saraf DN. Hydrocracking: a review. *Fuel* 1990;69:1467-73. DOI
195. Qi L, Peng C, Cheng Z, Zhou Z. Selective hydrocracking of poly-aromatics to mono-aromatics in a catalyst grading system of NiMo/Al_2O_3-HY and NiMo/Beta. *Fuel* 2023;351:128941. DOI
196. Qi L, Peng C, Cheng Z, Zhou Z. Structure-performance relationship of NiMo/Al_2O_3-HY catalysts in selective hydrocracking of poly-aromatics to mono-aromatics. *Chem Eng Sci* 2022;263:118121. DOI
197. Yu F, Zhang C, Geng R, et al. Hydrocracking of naphthalene over Beta zeolite coupled with NiMo/γ-Al_2O_3: investigation of metal and acid balance based on the composition of industrial hydrocracking catalyst. *Fuel* 2023;344:128049. DOI
198. Dik PP, Golubev IS, Kazakov MO, et al. Influence of zeolite content in NiW/Y-ASA-Al_2O_3 catalyst for second stage hydrocracking. *Catal Today* 2021;377:50-8. DOI
199. Lee D, Kim KD, Lee YK. Highly active and stable $CoWS_2$ catalysts in slurry phase hydrocracking of vacuum residue: XAFS studies. *J Catal* 2023;421:145-55. DOI
200. Vela FJ, Palos R, Trueba D, Bilbao J, Arandes JM, Gutiérrez A. Different approaches to convert waste polyolefins into automotive fuels via hydrocracking with a NiW/HY catalyst. *Fuel Process Technol* 2021;220:106891. DOI
201. Liu S, Kots PA, Vance BC, Danielson A, Vlachos DG. Plastic waste to fuels by hydrocracking at mild conditions. *Sci Adv* 2021;7:eabf8283. DOI PubMed
202. Sun G, Liu D, Li M, et al. Atomic coordination structural dynamic evolution of single-atom Mo catalyst for promoting H_2 activation in slurry phase hydrocracking. *Sci Bull* 2023;68:503-15. DOI PubMed
203. Brito L, Payan F, Albrieux F, Guillon E, Martens JA, Pirngruber GD. Hydrocracking of a long chain alkyl-cycloalkane: role of porosity and metal-acid balance. *ChemCatChem* 2023;15:e202201286. DOI

204. Dong Q, Zhang C, Zhang H, et al. Design and preparation of Pt@SSZ-13@β core-shell catalyst for hydrocracking of naphthalene. *J Catal* 2023;421:365-75. DOI
205. Saab R, Polychronopoulou K, Zheng L, Kumar S, Schiffer A. Synthesis and performance evaluation of hydrocracking catalysts: a review. *J Ind Eng Chem* 2020;89:83-103. DOI
206. Fan Y, Xiao H, Shi G, et al. Citric acid-assisted hydrothermal method for preparing NiW/USY-Al_2O_3 ultradeep hydrodesulfurization catalysts. *J Catal* 2011;279:27-35. DOI
207. Zepeda TA, Pawelec B, Obeso-estrella R, et al. Competitive HDS and HDN reactions over NiMoS/HMS-Al catalysts: diminishing of the inhibition of HDS reaction by support modification with P. *Appl Catal B Environ* 2016;180:569-79. DOI
208. Topsøe H. The role of Co-Mo-S type structures in hydrotreating catalysts. *Appl Catal A Gen* 2007;322:3-8. DOI
209. Lu Q, Chen CJ, Luc W, Chen JG, Bhan A, Jiao F. Ordered mesoporous metal carbides with enhanced anisole hydrodeoxygenation selectivity. *ACS Catal* 2016;6:3506-14. DOI
210. Singh NR, Delgass WN, Ribeiro FH, Agrawal R. Estimation of liquid fuel yields from biomass. *Environ Sci Technol* 2010;44:5298-305. DOI PubMed
211. Arora P, Abdolahi H, Cheah YW, et al. The role of catalyst poisons during hydrodeoxygenation of renewable oils. *Catal Today* 2021;367:28-42. DOI
212. Cordero-lanzac T, Rodríguez-mirasol J, Cordero T, Bilbao J. Advances and challenges in the valorization of bio-oil: hydrodeoxygenation using carbon-supported catalysts. *Energy Fuels* 2021;35:17008-31. DOI
213. Elliott DC, Hart TR, Neuenschwander GG, Rotness LJ, Zacher AH. Catalytic hydroprocessing of biomass fast pyrolysis bio-oil to produce hydrocarbon products. *Env Prog Sustain Energy* 2009;28:441-9. DOI
214. Cinibulk J, Vít Z. Hydrodenitrogenation of pyridine over alumina-supported iridium catalysts. *Appl Catal A Gen* 1999;180:15-23. DOI
215. Mendes FL, da Silva VT, Pacheco ME, Toniolo FS, Henriques CA. Bio-oil hydrotreating using nickel phosphides supported on carbon-covered alumina. *Fuel* 2019;241:686-94. DOI
216. Li H, Liu J, Li J, et al. Promotion of the inactive iron sulfide to an efficient hydrodesulfurization catalyst. *ACS Catal* 2017;7:4805-16. DOI
217. Budukva SV, Klimov OV, Uvarkina DD, et al. Reactivation of industrial NiMoP/Al_2O_3 hydrotreating catalyst: effect of orthophosphoric acid addition. *Appl Catal A Gen* 2020;592:117421. DOI